Winter 2021

Mixotrophy by Phytoflagellates in the Northern Gulf of Alaska: Impacts of Physico-Chemical Characteristics and Prey Concentration on Feeding by Photosynthetic Nano- and Dinoflagellates

Hana Busse
hana.busse@gmail.com

Mixotrophy by Phytoflagellates in the Northern Gulf of Alaska: Impacts of Physico-Chemical Characteristics and Prey Concentration on Feeding by Photosynthetic Nano- and Dinoflagellates

By

Hana Busse

Accepted in Partial Completion
of the Requirements for the Degree
Master of Science

ADVISORY COMMITTEE

Dr. Suzanne Strom, Chair

Dr. Kathryn Sobocinski

Dr. Shawn Arellano

GRADUATE SCHOOL

David L. Patrick, Dean

Master's Thesis

In presenting this thesis in partial fulfillment of the requirements for a master's degree at Western Washington University, I grant to Western Washington University the non-exclusive royalty-free right to archive, reproduce, distribute, and display the thesis in any and all forms, including electronic format, via any digital library mechanisms maintained by WWU.

I represent and warrant this is my original work and does not infringe or violate any rights of others. I warrant that I have obtained written permissions from the owner of any third party copyrighted material included in these files.

I acknowledge that I retain ownership rights to the copyright of this work, including but not limited to the right to use all or part of this work in future works, such as articles or books.

Library users are granted permission for individual, research and non-commercial reproduction of this work for educational purposes only. Any further digital posting of this document requires specific permission from the author.

Any copying or publication of this thesis for commercial purposes, or for financial gain, is not allowed without my written permission.

Hana Busse

2/25/2021

Mixotrophy by Phytoflagellates in the Northern Gulf of Alaska: Impacts of Physico-Chemical Characteristics and Prey Concentration on Feeding by Photosynthetic Nano- and Dinoflagellates

A Thesis
Presented to
The Faculty of
Western Washington University

In Partial Fulfillment
Of the Requirements for the Degree
Master of Science

by
Hana Busse
February 2021

Abstract

Long term monitoring in the Northern Gulf of Alaska (NGA) has shown that the high productivity of the region is closely coupled to lower trophic level food web dynamics. From previous observations of the NGA, we know that many nano- and dinoflagellates that compose this food web are mixotrophic, and therefore capable of both phagotrophy and phototrophy in a single cell. This behavior is believed to stabilize food webs by providing multiple pathways to energy and nutrients and may play an important role in the NGA, where environmental conditions are harsh and highly variable. To better understand the role of mixotrophic phytoflagellates in this region and how environmental factors drive mixotrophic behavior, field experiments and environmental sampling were conducted in summer and fall of 2019.

For the dinoflagellate, nanoflagellate, and cryptophyte communities there was a relationship between ingestion and environmental factors, with responses being specific to each taxonomic group. For the nanoflagellate community, a positive correlation between *Synechococcus* concentration and ingestion and a negative correlation between phosphate concentration and ingestion were observed. Alternatively, the dinoflagellate and cryptophyte communities responded to ambient light, where a negative correlation between ingestion and irradiance was observed. These differing responses indicate that phytoflagellates in the NGA are utilizing mixotrophy for both energy and nutrient acquisition and that differences are taxonomically specific. This initial study of small-celled mixotrophy highlights the prevalence and importance of this strategy in the NGA and indicates it may be a key contributor to overall ecosystem resilience and productivity.

Acknowledgements

Firstly, I want to thank my thesis chair, Dr. Suzanne Strom. Without her guidance, support, and insight this project would not have been possible. Suzanne and her super technicians, Kerri Fredrickson and Kelley Bright, encouraged me to problem solve and learn from experience while still be willing and able to answer any questions I had along the way. The research cruises in which this data was collected were made successful by Kerri's attention to detail and foresight and made fun by her positive attitude and sense of humor. I would also like to thank the crews and captains of the M/V Tiglax and R/V Sikuliaq and our collaborators at UAF for all of their hard work. I want to acknowledge the fellow grad students involved in the NGA LTER program and from SPMC who were there when seas got rough, specifically: Jake Lawlor, Annie Kandel, Clay Mazur, Kira Monel, and Megan Russell. Lastly, I would like to thank Brian Bingham, Kathryn Sobocinski, and Shawn Arellano for their thoughtful edits, R knowledge, and encouragement throughout my time at WWU. This research was funded by NSF (grant 1656070), NPRB (grants NA15MF4720173 and 1701) and WWU's office of Research and Sponsored Programs and Biology Department.

Table of Contents

List of Tables

List of Figures

Introduction

For decades, scientists have observed that many organisms classified as either phytoplankton or microzooplankton are both photosynthetic and phagotrophic (Stoecker et al. 2017). This mixotrophic capacity has originated independently in many protist lineages and is ubiquitous throughout the global oceans (Faure et al. 2019; Leles et al. 2017). In comparison with pure photo- or heterotrophy, mixotrophy has been shown to increase protist growth rates, photosynthetic ability, and winter survival (Flynn and Mitra 2009; Hansen et al. 2011; Millette et al. 2017; Schoener and Mcmanus 2017). Understanding how environmental conditions influence microplankton food webs is important for predicting ecosystem responses, particularly as global climate change alters precipitation, temperature and water column structure. Despite the observed prevalence of mixotrophy across lineages, until recently little was known about how communities utilizing this strategy respond to changes in environmental factors. The majority of field-based research on the subject focuses on individual species, rather than attempting to quantify mixotrophy at an ecosystem level.

Given the independent evolution of mixotrophy across clades, this strategy has likely evolved as a response to a variety of environmental drivers, and therefore may have distinct functional responses between taxonomic groups. In laboratory studies, for example, some species of dinoflagellates show increased feeding with increased photosynthetically active radiation (PAR) while others show the opposite response (Jeong et al., 2010; Li et al., 2000, Skovgaard et al., 2000). In nanoflagellates, ingestion has been shown to negatively correlate with phosphate in multiple studies, indicating ingestion may act as a nutrient acquisition mechanism rather than an energy acquisition mechanism for this group (Arenovski et al. 1995; Tsai et al. 2011).

Global models accounting for mixotrophy show higher trophic transfer efficiency and carbon flux, better aligning model output with in-situ results (Ward and Follows, 2016). Due to the potential diverse responses of mixotrophs to environmental drivers, there is a push for trait-based modeling approaches to be used when incorporating mixotrophy into biogeochemical and food web models (Flynn et al. 2013; Mitra et al. 2016). Broad estimates of mixotrophy do not allow us to fully understand how distinct taxonomic groups utilize this strategy; by pairing modeling efforts with studies that examine the functional responses of specific communities we are able to better depict lower trophic level dynamics. This approach not only better aligns models with food webs by accounting for mixotrophic behavior but also provides predictive power for the implications of this strategy in response to short-term and long-term environmental change.

In recent years, a shift towards small cell dominance along continental margins (Schmidt et al. 2019) may indicate that long term changes in environmental conditions would favor mixotrophic organisms, particularly small mixotrophs that are able to capitalize on increased bacterial prey concentrations and decreased microzooplankton predators. Nutrient uptake through phagotrophy allows primarily photosynthetic organisms to compete with primarily heterotrophic organisms during periods of low irradiance (Millette et al. 2017) or, alternatively, to enhance their nutrient acquisition – and hence growth rate – at high irradiances (Hansen and Nielsen 1997; Kim et al. 2008; Stoecker et al. 1997), depending on the mixotrophic strategy. The competitive success of these strategies is apparent in the number of bloom-forming mixotrophic species, including harmful algal bloom (HAB) species such as those responsible for paralytic shellfish poisoning occurrence in Alaska waters (Jeong et al. 2005).

Long-term monitoring efforts in the Northern Gulf of Alaska (NGA) have characterized the region's high variability in hydrological, chemical, and meteorological properties on seasonal, annual and interannual scales (Stabeno et al. 2004). These environmental conditions, and their variability, dictate the microplankton community structure and abundance (Strom et al., 2006; Strom et al., 2007), the effects of which propagate throughout the food web. In years when the spring bloom is absent or delayed the impacts can be observed in metazoan abundance and juvenile fish stocks in correlated years (Cavole et al. 2016; Hollowed et al; 2001; Pinchuk et al. 2008). Many of the organisms composing the base of this food web are known mixotrophs, with more suspected to be mixotrophic based on laboratory and field studies of nano- and dinoflagellates (Hansen et al. 2011; Jeong et al., 2010).

Mixotrophy has been observed as an important strategy for microzooplankton (ciliates, large dinoflagellates) in the NGA (Strom et al. 2020, in review). We believe the intense short-term environmental variability and strong seasonality of the region may select for mixotrophic nutritional strategies for both large (>20 μm) and small (<20 μm) cells. Freshwater input, highly variable weather patterns, complex bathymetry, and the presence of the alongshore Alaska Coastal Current (ACC) create a mosaic of distinct physical and chemical environments over short spatial and temporal scales. Light varies strongly in the water column on sub-daily to seasonal scales, leading to strong seasonality in photophysiology (Strom et al. 2016). Dissolved inorganic nutrients (DIN, e.g. nitrate, phosphate) can be limiting to at least some portions of the primary producer community on the NGA shelf, especially during the strongly stratified summer and (in some years) fall seasons (Strom et al. 2006). Mixotrophy may enable communities to better withstand these challenges stabilizing the base of the food web and, in part, contributing to the highly productive nature of the NGA.

In this study, links between phytoflagellate ingestion of the picocyanobacteria *Synechococcus* and the physical and chemical environment were explored through experimental approaches and by quantifying naturally occurring mixotrophs in the <20 µm photosynthetic community. This study aimed to not only quantify mixotrophy by phytoflagellates in the NGA but also begin to provide the insight needed to model this behavior for biogeochemical models of the region. Rather than focusing on a single species, a community approach was used to 1) determine if feeding by phytoflagellates on naturally occurring *Synechococcus* is linked to gradients in physical and chemical parameters, and whether these links vary by taxonomic group; 2) examine the feeding responses of constitutive mixotrophs of varying taxonomic groups to gradients in light availability, nitrate and phosphate concentrations, and prey availability; 3) quantify the proportion of the <20 µm summer and fall community that is capable of mixotrophy and obtain estimates of feeding rates within this size fraction.

Methods

This study had three main components: 1) an examination of ambient feeding by nano- and dinoflagellates in the NGA on naturally occurring *Synechococcus sp.*; 2) deckboard incubation experiments that examined the impacts of gradients in light, inorganic nutrients and prey concentration on ingestion; 3) an analysis of the composition of the <20 µm photosynthetic community in the summer and fall of 2019. These approaches were used in order to explore how environmental factors impact mixotrophic behavior on both broad scales and in regard to specific variables that are thought to be the primary drivers of mixotrophic behavior for phytoflagellates. Additionally, by determining the overall contribution of mixotrophic organisms to the <20 µm

community, we were able to gain an initial understanding of the importance of this strategy to the ecosystem as a whole.

Study Site and Environmental Characterization

This research was conducted as part of the NGA Long Term Ecological Research (LTER) program. All samples for this project were collected in 2019 during the summer cruise aboard the R/V Sikuliaq (June 26th to July 15th) and fall cruise aboard the M/V Tiglax (Sept. 10st -Sept. 26th). Five transects/regions were sampled during each cruise: the Seward Line (GAK), the Kodiak Line (KOD), Prince William Sound (PWS), the Middleton Line (MID) and the Copper River Plume region (PL, sampled in summer only) (Fig. 1). Inorganic nutrient samples were collected at every station, pre-filtered (0.8 μm), stored at -80°C and analyzed by the Aguilar-Islas laboratory at the University of Alaska, Fairbanks. Photosynthetically active radiation (PAR) data were collected using a deck-board PAR sensor (LiCor 2π). Temperature and salinity values were collected from CTD sensors at the same depth as sample collection. All statistics were completed using R Statistical Software (R Core Team, 2020).

Ambient Feeding Measurements

To examine ambient feeding by phytoflagellates on naturally occurring *Synechococcus* samples were taken at 25 stations during summer and 10 stations during fall (Table 1). Samples collected from the 50% light level (~4 m) using a standard CTD rosette, fixed with 0.5% glutaraldehyde, DAPI-stained to facilitate identification of dinoflagellates by their distinctive nuclei, filtered using 2 μm (summer) and 0.8 μm (with 1.2 μm backing) (summer, fall) polycarbonate filters, slide-mounted with low fluorescence immersion oil, and frozen (-80°C) for transport on dry ice to Shannon Point Marine Center (Kemp et al., 1993). At stations where both

pore sizes of filters were used enumeration of ingestion was completed on each and compared; there was no significant difference between ingestion estimates across the two pore sizes (t-test, p=0.72, 12 df). Thus, data from both pore sizes were combined for analysis.

Samples were analyzed to quantify mixotrophic activity using epifluorescence microscopy; preservation and microscopy methods for <20 μm protists are from Strom et al. (2016). All samples were analyzed within 6 months of sample collection. Species-level identification was not possible using this technique; rather, general taxonomic categories of dino- and nanoflagellates were used. Groups sufficiently abundant for mixotrophic enumeration included miscellaneous nanoflagellates at every station and *Gymnodinium*-type dinoflagellates at some stations. Additionally, cryptophytes were enumerated for mixotrophic ingestion in fall samples.

Overall cell shape and presence of chloroplasts was used to identify phototrophic dinoflagellates (Fig. 2A) in conjunction with their distinctive large nuclei and condensed chromosomes observable under ultraviolet illumination. Nanoflagellates were identified by size and presence of red autofluorescent chloroplasts under blue light illumination (Fig. 2B). Cryptophytes are distinctive from other nanoflagellate groups due to orange autofluorescent pigments (Fig. 2C). In Figure 2 (A, B) you can see ingested *Synechococcus* fluorescing yellow, allowing for the enumeration of ingested cells within phytoflagellates. For each abundant dinoflagellate and nanoflagellate taxon, 50 individuals per slide were counted and the number of ingested *Synechococcus* prey per cell was recorded. The number of cells with ingested prey was divided by the total counted (n=50), resulting in an estimate of the fraction of cells feeding per taxon.

Correlations between environmental variables and feeding were completed using Kendall's tau ranked correlation tests. This correlation test was used due to the small sample sizes and tied ranks present in the data. Prior to analysis correlations between environmental variables were tested and highly correlated variables were reduced in order to remove redundancy (Supplemental Table 2). The final variables examined in relation to ingestion were salinity, temperature, PAR, nitrate, phosphate, ammonium and *Synechococcus* concentration. All were centered (means subtracted) and scaled (values divided by their standard deviation) prior to analysis. PAR data was scaled to collection depth using the attenuation coefficient at each station. Light history intervals of 4h, 8h, 12h, 16h, and 24h were tested by totaling the scaled deck-board PAR over the time interval prior to sampling. Environmental factors were examined with principal component analysis (PCA) to determine whether there was any clustering or ordination associated with high/low ingestion or season and generalized linear modeling approaches were employed to explore the impacts of specific parameters on the ingestion patterns observed.

Deckboard Incubation Experiments

In summer 2019, we conducted parallel 4-h experiments testing the effect of PAR, DIN, and prey concentration on ingestion of *Synechococcus* by nano- and dinoflagellates. Water was collected from the 50% light level, screened through 150 μm mesh and distributed into 250-mL polycarbonate bottles using silicone tubing, gentle handling techniques, and regular mixing. Experiment bottles were kept in a temperature-controlled environment with limited light exposure while the three treatments were applied. After treatment addition, bottles were incubated in flowing seawater-cooled deck incubators to provide natural light and temperature conditions (experimental setup further outlined in Supplemental Fig. 1).

PAR and DIN gradient experiments were conducted at 7 sites throughout the cruise (Table 1). To obtain gradients in PAR, neutral density screen and black tape was used to cover the experimental bottles creating 5 light levels: 100, 50, 30, 10, and 0% of full sun irradiance. For DIN experiments, bottles were left unenriched (ambient DIN) or were inoculated with $NaNO_3$ to achieve approximate enrichments of 0.5, 1.0, 2.0, 4.0, and 8.0 µM NO_3. For each treatment phosphate was added in addition to $NaNO_3$ to achieve Redfield ratios (N:P=16:1). These additions were chosen based on the observed range of nitrate concentrations in the NGA, with expected near-surface NO_3 concentrations in summer ≤0.2 µM (Strom et al., 2006; Aguilar-Islas, unpublished data). For both PAR and DIN experiments two bottles were incubated per treatment level. All bottles in the DIN experiments were screened to the 50% light level using neutral density screen bags to maintain collection depth light conditions. Cultured high latitude *Synechococcus* sp. cells were added in both experiments to create prey-saturated conditions ($5x10^4$-$6x10^5$; see below for culture methods).

Cultured *Synechococcus* sp. (strain MICROVIR 16CR_2_clonal) was grown at $1.8x10^{15}$ (quanta $cm^{-2}s^{-1}$) and 15°C at SPMC with a 12h light-dark cycle and maintained in similar conditions aboard the R/V Sikuliaq. This high-latitude North Atlantic strain was obtained from the Roscoff Culture Collection (RCC # 3010). The culture was grown using SN media (Waterbury et al. 1986, with Red Sea salts replacing filtered seawater) in glass 1L bottles and transferred every 2-3 weeks depending on culture thickness. To reduce nutrient carry-over associated with the culturing medium, cultured *Synechococcus* was centrifuged, (2,500 rpm, 10 min) and resuspended in local seawater that had been filtered using a 0.45 µm glass fiber filter. To determine prey concentrations prior to inoculation, epifluorescence microscopy and a counting grid were used; spiking volumes were calculated based on cell concentrations.

Prey concentration experiments were conducted at 5 of the 7 experimental sites. Prey concentration gradients were created by adding various amounts of cultured *Synechococcus* ranging from 0 - $1x10^6$ cells ml^{-1} to experiment bottles. This range was based on naturally occurring *Synechococcus* observed in the NGA during summer and fall months (Strom, unpublished), with the highest treatment level exceeding natural conditions. Bottles were screened to the collection light level (~50% ambient PAR) using neutral density screening and no nutrients were added. Five treatment levels were used with two bottles incubated at each treatment level.

After the 4 h incubation period, 100 ml subsamples from each bottle were fixed, stained, and filtered onto 2 µm pore size, slide-mounted, and frozen in the same manner as the ambient feeding measurement samples. Additionally, the microscopy methods were the same for both the ambient feeding measurements and grazing experiments. Nanoflagellates were present at abundances sufficient to be enumerated at every experimental site while dinoflagellates were only sufficiently abundant at 2 of the 7 stations.

Initial samples with and without added *Synechococcus* were compared to determine if there was any adherence of added *Synechococcus* to cell exteriors; this could mimic ingestion and skew results. No difference was observed ($p= 0.52$, 12 df), indicating that *Synechococcus* adhering to the outside of grazer cells was not artificially elevating our ingestion estimates. Additionally, samples with and without added prey at the end of the 4 h incubation period were compared to assess if the natural nano- and dinoflagellate community was ingesting the added cultured *Synechococcus* sp. Ingestion estimates showed increased spread and higher mean in the samples treated with cultured *Synechococcus* (Fig. 3) indicating that at least part of the community showed increased ingestion in response to the added prey.

Ambient light, DIN and *Synechococcus* cell concentrations for each experimental site are outlined in Table 1. Nutrient samples were taken from five bottles per set of experiments: the initial water sample with no addition; a pre-incubation sample with nutrient stock added to achieve 2.0 µM nitrate; a pre-incubation sample with cultured *Synechococcus* added to achieve $5x10^5$ *Synechococcus* cells ml^{-1} concentration; a post-incubation sample with no prey or nutrient addition; and a post-incubation sample that received both the 2.0 µM nitrate treatment and the above *Synechococcus* addition. The nutrient concentrations from these samples along with the known volumes of nutrient and prey additions were used to estimate the nutrient profile for each bottle in all experiments.

For each set of treatments (DIN, PAR or prey concentration), responses were examined and when there appeared to be a response an appropriate functional response curve or linear model was tested. The final values used for visualization and analysis for each treatment included the ambient PAR, DIN or *Synechococcus* concentration plus the *Synechococcus* additions, DIN additions and light screening added to create the final treatment gradients (post addition treatment values for each set of experiments are outlined in Supplemental Table 1).

Community Composition Analysis

To determine the overall contribution of mixotrophic organisms to the <20 µm community the community composition was determined at each station sampled. Samples were filtered unto a 0.8 µm polycarbonate filters using a backing filter to ensure even cell distribution. Filters were then slide-mounted and stored at -80°C until community composition analysis was completed. Only organisms containing observable chloroplasts were recorded. Organisms <10 µm were examined at 1000x under oil immersion using a $0.01mm^2$ grid to determine

approximate cell size and shape and determine number of cells per grid counted. Grids counted were chosen randomly across the slide. Transects at 400x were used to count cells in the 10-20 μm range and were conducted until ~50% of the slide had been counted or n=20 of one taxon.

For each sample, the volume filtered, total slide area, and total area counted were used to calculate approximate abundances of cells L^{-1} for each size and taxonomic category. Cell biomass for *Synechococcus* cells was assumed to be 200 fgC/cell (Heldal et al. 2003, Liu et al. 1999, Stramski et al. 1995). For larger cells the cell shape (oblong or round) and size was used to estimate cell volume (BV μm^3); volume was converted to biomass (pgG) according to logC = -0.363 + 0.863(logBV) (Verity et al., 1992).

The organisms observed to be mixotrophic in this study, including nanoflagellates, *Gymnodinium*-type dinoflagellates, and cryptophytes, were recorded separately in the community composition analysis. This allowed for estimation of the percent contribution of mixotrophs to the <20 μm photosynthetic community by taxonomic group and by size class. The final taxonomic groupings included *Synechococcus*, picoeukaryotes, nanoflagellates, cryptophytes, miscellaneous autotrophic flagellates, miscellaneous autotrophic dinoflagellates, Gymnodinium-type dinoflagellates, and diatoms. The size classes examined were 0-2.5 μm, 2.5-5 μm, 5-10 μm, 10-15 μm, and 15-20 μm. To test for relationships between community composition structure and environmental variables a PCA approach was utilized. Size class and taxa groupings were analyzed separately, and any clustering or ordination observed was examined to determine if it corresponded to variability in salinity, temperature, or nutrient environment.

Results

Environmental Conditions and Seasonality

Large variations in physico-chemical factors were observed across the NGA sampling area and between the summer and fall seasons (Table 1). As expected, cross shelf gradients in salinity (lower near shore) and macronutrients (higher offshore) were present along the GAK line, especially in fall. In the Copper River plume (PL) study area we saw changes in salinity and macronutrients over short spatial scales due to large amounts of freshwater discharge from the Copper River and complex patterns of mixing with shelf waters. We measured anomalously high sea surface temperatures in the summer that persisted into the fall, with summer temperatures ranging between 11.6° C and 17.7° C and fall temperatures ranging between 11.2°C and 14.7° C. The fall cruise was also marked by a distinct decrease in daily PAR and an increased mixed layer depth. Despite these seasonal differences in environmental conditions, the degree to which the mixotrophic flagellate community was observed with ingested *Synechococcus* prey cells remained consistent, with an average of 12% of the total community (nanoflagellates and dinoflagellates combined) feeding in the summer and 15% feeding in the fall.

When principal component analysis was used to assess patterns in environmental variability and how they relate to season, location, and ingestion, the drivers of the first two principal components were easily defined and accounted for a combined 54% of the total variance (Fig. 4, Table 2). The first principal component appears to correspond to degree of stratification given that there was separation with respect to salinity, macronutrients, and temperature, while separation on PC 2 represents seasonality driven by differences in PAR levels, ammonium, and (to a lesser extent) *Synechococcus* concentrations. The biplot created by

overlaying fraction nanoflagellate feeding on the environmental PCA showed weak ordination across both PC1 and PC2, with increased feeding occurring where there was higher stratification and summer-like conditions (Fig. 4B). There were no clear groupings based on region sampled (i.e. PWS, Copper River) or location on shelf (i.e. nearshore/offshore).

Ambient Feeding Measurements

Responses to light history and PAR varied by the community examined, but longer light history intervals yielded stronger correlations. The fraction feeding for dinoflagellate and cryptophyte communities was negatively correlated with PAR (Fig. 5A, B); in contrast, there were no significant correlations for the nanoflagellate community. We examined light history intervals of 4, 8, 12, 16 and 24 h by totaling hourly PAR over that period prior to sample collection and found that there was no significant relationship with feeding for any community when a period of less than 24 h was utilized. The relationship between ingestion and PAR was stronger for the cryptophyte community (τ= -0.9, p=0.003) than the dinoflagellate community (τ= -0.41, p=0.027), though it should be noted that there was a smaller sample size for cryptophytes (n=7) given that they were only assessed in fall samples.

Both nanoflagellate and dinoflagellate ingestion were related to environmental factors in addition to PAR. For the dinoflagellate community, there was a negative correlation between ingestion and temperature (τ= -0.42, p=0.02) (Fig. 5C) and for the nanoflagellate community, there was increased feeding at stations with more *Synechococcus* (τ=0.2, p=0.06) (Fig. 5D) and decreased feeding at stations with higher phosphate concentrations (τ= -0.2, p=0.06) (Fig. 5E). Ambient ingestion by nanoflagellates was related to both prey and phosphate concentrations, with high levels of ingestion only occurring where *Synechococcus* concentrations were high and

ambient phosphate was low (Fig. 6). Additionally, we tested salinity, nitrate, and ammonium and saw no significant correlations with ingestion for any of the mixotroph groups examined (Supplemental Table 3). All correlation analysis included both summer and fall samples and used an alpha of 0.1 to reduce chances of a Type II error given the small sample sizes.

Responses were additionally tested using generalized linear models (GLMs) with model inputs chosen based on the results of the correlation analyses, but no significant relationships were observed for any of the taxonomic groups examined. The lack of significance when using a GLM approach compared to a correlation approach was likely due to high variability between replicates and the small sample sizes obtained (n=33 for nanoflagellates, n=19 for dinoflagellates, n=9 for cryptophytes). A model including all taxonomic groups, with group as a factor, was also tested without significant results.

Deckboard Incubation Experiments

In addition to variability in ambient levels of PAR and macronutrients across the study area in the summer (Table 1) there were also notable differences in station-to-station community composition that impacted enumeration for the deckboard experiments. Nanoflagellates were observed at every station in relatively high abundance (6.0×10^2 - 1.6×10^3 cells/ml) while autotrophic dinoflagellates were only abundant (3.1- 18.3 cells/ml) at PWS 2 and GAK 15. The autotrophic dinoflagellates we did observe were 7-8 µm round and oblong *Gymnodinium*-type cells. The nanoflagellates present were primarily prymnesiophytes and unidentified round nanoflagellates, and they were consistently abundant enough to enumerate in both summer and fall. Within each category, nano- or dinoflagellate, two subgroups (nanoflagellates: prymnesiophytes, unidentified round cells; dinoflagellates: round and oblong *Gymnodinium*-type

cells) were initially counted separately but then were combined for analysis due to similar feeding responses. Given the small sample sizes and morphologically distinct sub-group types, differences in feeding responses among stations may be a function of taxon or ambient environmental conditions rather than treatment.

Dinoflagellates had higher overall average feeding levels, ranging from 0.16 to 0.24 compared to 0.04 to 0.18 for the nanoflagellates. For both communities, nano- and dinoflagellates, the highest ingestion was observed at PWS 2 (Fig. 7). Differences in average ingestion across experimental sites may be linked differences in ambient phosphate across stations, given that there was increased feeding observed when phosphate was low. When examined separately, stations with lower phosphate concentrations (<0.4 μM) showed generally higher levels of ingestion within the nanoflagellate community for both the DIN and PAR experiments (Fig. 8). Additionally, stations with lower ambient phosphate showed increased nanoflagellate responses to light treatments (Fig. 8). Dinoflagellates also showed no relationship with DIN (Fig. 9A) and no clear increase in fraction feeding with PAR dose (Fig. 9B) although the highest feeding was observed in the experiment with the largest amount of PAR received. Dinoflagellates were only enumerated at stations that were later determined to be low ambient phosphate stations.

Mixotroph feeding during deckboard experiments increased in response to *Synechococcus* concentration, though the response curves for nanoflagellates and dinoflagellates look quite different. The nanoflagellate feeding response to increased *Synechococcus* concentration when ship-board experiments were combined (Fig. 10A) was described well by the Michaelis-Menten predator-prey response relationship FF = (FFmax*Syn)/(k+Syn) where FF = fraction feeding, FFm = maximum fraction feeding, Syn = *Synechococcus* concentration

(cells/ml), and k = half-saturation constant (cells/ml) (Holling 1959, Holling 1965). FFmax was 0.15 and the half-saturation constant was $1.01x10^5$ cells/ml (Fig. 10A, Residual Standard Error = 0.023, df = 48). The only station where prey addition experiments were conducted that there was a large enough dinoflagellate community to enumerate was GAK 15. At that station we saw a significant linear increase in the fraction feeding for the dinoflagellate community as *Synechococcus* concentration increased ($p=0.017$, df=8, $R^2=0.53$) (Fig. 10B).

Community Composition Analysis

The summer biomass was dominated by small cells, particularly *Synechococcus* and picoeukaryotes, with the highest *Synechococcus* biomass observed at GAK 9 (96.0 µgC/L, $4.8x10^5$ cells/ml), PL 7 (73.0 µgC/L, $3.7x10^5$ cells/ml) and PL 10 (58.8 µgC/L, $2.9x10^5$ cells/ml) (Fig. 11A). There was an increase in *Synechococcus* with increasing distance offshore until GAK 9 (166.68 km offshore) then a decrease at GAK 15, seaward of the shelf break. In the fall there was still a high proportion of small cells but a decrease in overall *Synechococcus* biomass, with the highest biomass (41.5 µgC/L) and abundance ($2.1x10^5$cells/ml) observed at PWS 1 (Fig. 11B). There was a wide range of nanoflagellate biomass and abundance in the summer samples (3.1 to 30.0 µgC/L, $7.5x10^2$ to $4.7x10^3$ cells/ml), with the lowest levels observed in PWS and the Copper River Plume. Fall nanoflagellate biomass and abundance was relatively constant at every station sampled (13.3 to 26.9 µgC/L, $2.4x10^3$ to $5.5x10^3$ cells/ml). Autotrophic dinoflagellate biomass increased seasonally from an average of 0.2 µgC/L in the summer to an average of 0.6 µgC/L in the fall (including both mixotrophic *Gymnodinium*-types and miscellaneous autotrophic dinoflagellates).

Across both seasons the 10-20 µm size class was a minor contributor to biomass (average 2.3 µgC/L in summer, 2.6 µgC/L in fall) with most cells occupying the <5 µm size fraction (Fig. 12). The increase in fall is due to a doubling of the autotrophic dinoflagellate biomass (0.29 to 0.63 µgC/L), which enabled the enumeration of mixotrophy dinoflagellates in the fall samples. The fall samples also contained a much larger proportion of 2.5 – 5 µm cells, largely due to an increase in miscellaneous autotrophic flagellates, particularly at PWS 2. There were no strong cross-shelf patterns observed with regard to size class in either season.

When using PCA to examine the community composition we saw that clustering of picoeukaryotes and miscellaneous autotrophic flagellates, and also of cryptophytes and nanoflagellates (Fig. 13A). The close grouping of picoeukaryotes and miscellaneous autotrophic flagellates may indicate overlap between these two groups that was missed with the level of identification possible using epifluorescence microscopy, but lack of separation during microscopy would not explain the grouping of cryptophyte and nanoflagellates, which have distinctive autofluorescent properties. Flagellates (all types) and diatoms both separated from *Synechococcus* on PC1.There was no clear clustering or ordination of taxonomic groups with regard to season (Fig. 13A) or in conjunction with other environmental variables that were examined using biplots (not pictured).

When a similar PCA was conducted using size class rather than taxonomic group we again saw clear separation of *Synechococcus.* There was clustering of 0-2.5 and 2.5-5 µm cells, and of 10-15 and 15-20 µm size classes (Fig. 13B). The <5 µm organisms include the picoeukaryotes and misc. autotrophic flagellates, which also grouped in the taxonomic PCA, but also include nanoflagellates and cryptophytes which were grouped with each other but clearly separated from the picoeukaryotes and misc. autotrophic flagellates in the taxonomic analysis.

The 10-15 size class contained a mix of dinoflagellates and diatoms while the 15-20 µm size classes contained mostly diatoms, likely contributing to their clustering. When PCA scores are coded according to temperature (Fig. 13C) we observed lower temperatures in association with stronger influence of the 10-15 and 15-20 µm size classes, highlighting the role of temperature as an important driver for size structure in the <20 µm community. There were no clear patterns between salinity and DIN and PCA scores.

The average proportion of the photosynthetic community observed to be mixotrophic was roughly constant across season, 0.27 in summer and 0.29 in fall, but varied dramatically by station (Fig. 14A, B). The highest proportions of mixotrophy were observed at KOD 3, GAK 15, and PL 4 in the summer and GAK 5 in the fall (Fig. 14A, B). Mixotrophic flagellates as a proportion of total flagellates (rather than the total <20 µm photosynthetic community) was much higher in the summer (average 0.64) than the fall (average 0.43) (Fig. 14C, D). Organisms were grouped as mixotrophic flagellate, autotrophic flagellate or non-flagellate (i.e. *Synechococcus* and Diatom) based on direct observation of ingested *Synechococcus* in this study.

Discussion

Overview

Mixotrophy by phytoflagellates in the NGA was tied to abiotic and biotic conditions and is likely a critical strategy for the <20 µm plankton community. Responses to environmental variables by mixotrophic flagellates were taxon-specific, with dinoflagellates, cryptophytes, and smaller nanoflagellates exhibiting varying and sometimes contrasting responses to phosphate, light availability, prey concentration, and temperature. Overall, the nanoflagellate community

appeared to be relying on mixotrophy as a means of nutrient acquisition while the dinoflagellate and cryptophyte community relied on ingestion as an energy acquisition mechanism in times of low irradiance.

At a given station up to 90% of the small phototrophic flagellates in the NGA were utilizing mixotrophy, with the average across summer and fall being 63% and 43% respectively. This first study of phytoflagellate mixotrophy provides initial insights into community-level ingestion by dinoflagellates, cryptophytes, and smaller nanoflagellates. Given the methods used, these are approximations – and likely underestimates - of mixotrophic flagellate feeding. As we continue to learn about the community composition of this area and the physiology and behavior of the organisms that inhabit it, models that better capture the complex dynamics at the base of this food web can be built. These models, in turn, can be used to determine the ecosystem-wide role of mixotrophy in supporting resilience and stability in the NGA

Community-Level Ingestion Responses

1. Dissolved Inorganic Nutrients

Previous studies have shown similar negative correlations between phosphate concentration and ingestion within nanoflagellate mixotrophs (Livanou et al. 2019; Sato et al. 2017; Tsai et al. 2011; Unrien et al. 2007). Our results revealed ambient feeding was negatively correlated with phosphate concentration, and experiments conducted at stations with lower ambient phosphate (i.e. <0.4 μM) revealed higher levels of nanoflagellate feeding, despite treatment. The common hypothesis for this relationship is that ingestion provides a nutrient acquisition mechanism in times of low ambient phosphate (Arenovski et al. 1995; Duhamel et al. 2019; Tsai et al. 2011). Macronutrient limitation has been observed in the NGA in summer

months (Strom et al. 2006) but nitrate is believed to be the limiting factor to phytoplankton growth rather than phosphate.

In examinations of the relationship between phosphate and nanoflagellate feeding Duhamel et al. (2019) found that PO_4 uptake rates in mixotrophic nanoflagellates saturated at phosphate concentrations of 0.011 to 0.038 μM depending on taxonomic group. Phosphate concentrations in the NGA exceeded these even during summer months when the water column was highly stratified (Table 1). These uptake rates may be ecosystem- or species-specific but in conjunction with previous studies examining macronutrient limitation on the NGA shelf, it seems phosphate concentrations are likely not limiting phytoplankton growth in the NGA. Therefore, there may be another driver behind the relationship between phosphate and mixotroph feeding. For example, phosphate could co-vary with another key nutrient, or act as a signaling mechanism triggering feeding within the cell.

It is well established that phytoplankton growth in the offshore NGA region is iron limited (Boyd et al. 2004; Martin and Fitzwater 1988) and that iron input as a result of glacial runoff or dust deposition are quickly bound by organic ligands (Aguilar-Islas et al. 2010; Aguilar-Islas et al. 2016). Dissolved iron concentrations on the shelf have been shown to be potentially limiting as well, with concentrations as low as 0.2 nM in July and 0.07 nM in August (Koch et al. 2011, Wu et al. 2009). Vitamin B_{12} has also been shown to be low (0.1-3.8 pM) across the NGA shelf and positively correlated with phosphate concentration (Koch et al. 2011). This relationship highlights the possibility that phosphate could be co-varying with a key micronutrient or vitamin that was not tested in this study, potentially one that it commonly covaries with given that the phosphate-ingestion relationship has been observed in other ecosystems. In this study, correlations between phosphate and nitrate, nitrite, temperature, and

salinity (Supplementary Table 2) were observed, though none of those additional environmental factors correlated significantly with fraction of the community feeding.

Phosphate is crucial for cell functioning, as a key component in RNA, DNA, and ATP (Lin et al. 2016). The essential role of phosphate in the cell may allow for intracellular phosphate concentration to act as a signaling mechanism triggering grazing behavior. Internal phosphate concentrations have been shown to impact dinoflagellate *Ceratium furca* ingestion (Smalley et al. 2003) but have not been studied in nanoflagellates specifically. The link between phosphate concentration and ingestion by mixotrophic nanoflagellates needs to be examined more thoroughly in the laboratory setting, especially since that link has been documented across multiple ecosystems with distinct physico-chemical environments and communities of nanoflagellates (Duhamel et al. 2019; Livanou et al. 2019; Sato et al. 2017; Tsai et al. 2011; Unrien et al. 2007).

2. Synechococcus Concentration

Few experimental studies examining mixotrophic nanoflagellate ingestion and prey concentration have been conducted but correlations between ingestion and *Synechococcus* concentration have been observed previously from in situ observations, similar to our ambient feeding results (Chan et al. 2019). The half-saturation constant for *Synechococcus* ingestion by nanoflagellates was 1.01×10^5 cells/ml when fit with a Michaelis-Menten functional response curve (Fig. 10). Using this value, 8/15 stations in the summer and 2/10 stations in fall can be classified as prey saturated for the nanoflagellate community.

At prey saturated stations (ambient *Synechococcus* $>2.0 \times 10^5$) there was still a 3x range in feeding level, highlighting that *Synechococcus* ingestion by nanoflagellates was only partially

controlled by encounter rate. At stations with a high concentration of *Synechococcus* and relatively high ingestion (>0.12 fraction of cells feeding), there was low (<0.4 μM) ambient phosphate present. These results indicate that the nutrient environment was likely the primary driver dictating nanoflagellate ingestion (Fig. 6), though more complicated trophic interactions between mixotrophic nanoflagellates and *Synechococcus* may be occurring. *Synechococcus* sp. are able to outcompete nanoflagellates for dissolved macronutrients (Duhamel et al. 2019); increased *Synechococcus* therefore may lead to decreased ambient phosphate concentrations driving an increase in grazing by nanoflagellates. In this scenario, grazing would both provide phosphate to nanoflagellate cells and decrease nutrient competition. A negative correlation between *Synechococcus* concentration and phosphate concentration was not observed in this study, though that could have been due to the small sample size (n=25) obtained.

For the mixotrophic dinoflagellate community, there was also a positive relationship between *Synechococcus* concentration and fraction feeding in the deckboard experiment completed. Contrary to the nanoflagellate community, we saw a linear relationship rather than a Type-II predator-prey functional response (Fig. 10). Multiple ingested prey cells were seen more frequently within individual dinoflagellate cells than within nanoflagellates. In conjunction with their larger size, this may indicate that a larger prey population would be necessary to saturate dinoflagellate feeding, explaining why we only saw a response in our experimental results and not in the ambient feeding analysis. Photosynthetic dinoflagellate ingestion rates have been shown to increase with *Synechococcus* concentration in previous work (Jeong et al. 2005), with ingestion rates varying depending on dinoflagellate species. When prey saturation levels were examined, dinoflagellate ingestion was saturated at *Synechococcus* concentrations of 1.1-1.4 x 106 cells/ml (Jeong et al. 2005). These concentrations exceed the ambient levels of

Synechococcus observed across the shelf in this study and are only reached by the highest treatment level in the prey concentration experiment (Table 1, Fig. 10 B).

Mixotrophic dinoflagellates are known to ingest many types of prey in addition to *Synechococcus* (Jeong et al. 2010). An examination of the >20 µm mixotrophic dinoflagellate community in the NGA by Strom et al. 2020 (in review) and their ingested prey revealed a complex food web of mixotrophic organisms grazing upon other mixotrophic organisms, with grazing on cyanobacteria still common among large dinoflagellates. Dinoflagellates in the < 20 µm size class also likely consume many types of prey (Jeong et al. 2010) and it may be that ingestion in the NGA was closely coupled to prey types not examined in this study, which could have influenced dinoflagellate feeding rates on *Synechococcus*. The complex trophic dynamics at the base of marine food webs are challenging to untangle. Future studies examining dinoflagellate feeding in this region should include grazing on cryptophytes, haptophytes, and chlorophytes in addition to cyanobacteria to see if preferential grazing is occurring and how those rates may be impacted by environmental factors.

3. Light and Temperature

Ingestion by mixotrophs is thought to function as either a means of carbon (i.e. energy) acquisition or nutrient acquisition (Stoecker et al. 2017). In the first scenario, feeding is expected to increase in response to decreased light availability, allowing the organism to gain energy through phagotrophy rather than phototrophy in times of low irradiance. In the second scenario, feeding is expected to increase when there is more light and conditions are conducive to population growth, with ingestion providing the key nutrients required. Therefore, the relationship between feeding and light availability can be hard to classify as increases and

decreases in feeding by both nanoflagellates and dinoflagellates have been observed (Andersen et al. 2017; Chan et al. 2019; Jeong et al., 2010; Li et al., 2000, Skovgaard et al., 2000).

Our results show that ingestion by mixotrophic nanoflagellates was not strongly related to PAR in either the deck-board incubation experiments or the ambient samples. In contrast, ingestion by both cryptophytes and dinoflagellates was negatively correlated with ambient PAR when a 24h light history interval was used (Fig. 5), for the cryptophyte community this trend was particularly noticeable with a correlation coefficient of -0.91 and a p value of <0.005. These differences across trophic groups strongly suggest that there are multiple, contrasting mixotrophic strategies being utilized by organisms in the NGA. Feeding by photosynthetic nanoflagellates seems to be primarily driven by the need for nutrient acquisition while dinoflagellates and cryptophytes may be using ingestion to gain energy in times of low irradiance.

When shorter light history intervals were tested (4h, 8h, 12h, 16h) there was no relationship between ingestion and PAR for either the dinoflagellate or cryptophyte communities, signifying an acclimation period is necessary before changes in light availability translate to feeding. This acclimation period may play an important role in determining how organisms respond to environmental variability, given that on a diel cycle PAR can change rapidly due to changes in weather and mixed layer depth. The apparent 24-h acclimation time frame could explain the lack of substantial feeding responses in our deckboard PAR experiments, which were conducted using a 4 h incubation period.

In addition to PAR, ambient sampling revealed a negative correlation between temperature and dinoflagellate ingestion. The presence of distinct dinoflagellate species at

different stations and across the two seasons sampled could also have contributed to this correlation. In contrast to our findings, laboratory studies of mixotrophic dinoflagellates have shown increases in ingestion associated with increased temperatures to a point, and then decreases once temperatures become extreme (Jeong et al. 2018, Kang et al. 2020). Jeong et al. saw a positive relationship between ingestion and temperature in the dinoflagellate *Paragymnodinium shiwhaense* up to temperatures of 20 C° and Kang et al. saw a similar pattern in dinoflagellate *Yihiella yeosuensis* up to 30 C°, highlighting the species-specific nature of these relationships.

The temperatures observed across the NGA in summer and fall 2019 ranged between 11-18 C°; this is below the level in which reduced feeding was observed in laboratory studies but anomalously high for this ecosystem, even in summer months (Litzow et al. 2020). Due to the high temperatures observed, the dinoflagellate community may have been at the top of its optimal temperature threshold for ingestion and reduced ingestion at higher temperature stations may have been due to heat stress. Temperature also correlated with salinity, nitrite, nitrate, and phosphate, and therefore this relationship could have emerged as a consequence of one of these factors, though none of them individually correlated with dinoflagellate ingestion.

Mixotrophy in the NGA

1. Significance of Mixotrophy in <20 µm Cells

Though mixotrophy by nanoflagellates, cryptophytes, and dinoflagellates is well established (Stoecker et al. 2017, Unrein et al. 2014), quantification of mixotrophy by small cells is largely undocumented across much of the global ocean, including the NGA prior to this study. Of the <20 µm phytoflagellate community present in summer and fall 2019, the proportion

mixotrophic ranged from an average of 0.64 (summer) to 0.43 (fall) and of the total <20 μm community, including non-flagellates, the proportion mixotrophic was 0.27 (summer) and 0.29 (fall) (Fig. 14). These high proportions within both the total <20 μm size class, and especially within the phytoflagellate community, highlight the critical role of this strategy in the NGA.

This account of mixotrophy is likely an under-representation given that mixotrophy was only quantified when we directly observed ingestion of *Synechococcus* by a chloroplast-containing cell. Therefore, the ingestion of heterotrophic bacteria or eukaryotes was not accounted for (Beisner et al. 2019). The use of epifluorescent microscopy for taxonomic groupings also means that only rough classifications could be made, and that some organisms classified as miscellaneous autotrophic flagellates may have belonged in the mixotrophic nanoflagellate category and vice versa.

2. Seasonality and Small-cell Dominance

Despite distinct weather changes between summer and fall, the environmental conditions and community composition were similar across the two seasons sampled. Based on temperatures and macronutrient concentrations, it appears that the beginning of the fall cruise (September 12th- September 17th) was capturing late summer conditions. The transition to fall conditions began on September 19th (during sampling at GAK 9) as a low-pressure system entered the study area and wind mixing increased.

Mixotrophic phytoflagellate ingestion has been shown to vary by season, peaking in warmer months (Chan et al. 2009). Given that we weren't able to fully capture differences between summer and fall conditions, the ingestion observed in this study likely corresponds to peak annual ingestion of these communities. Increased mixotrophic dinoflagellate biomass in the

> 20 µm size class has also been observed in summer months (Strom et al. 2020, in review). Previous studies have shown that during spring conditions, diatoms with higher surface area to volume ratios can outcompete flagellates when nutrients are abundant. Then, as the water column becomes stratified and nutrient levels drop, mixotrophs are able to dominate (Cadier et al. 2020).

Previous work has shown that mixotrophy is common in microzooplankton communities across the NGA (Strom et al. 2020, in review). Both ciliates that use stolen chloroplasts to photosynthesize and dinoflagellates capable of stretching to consume large chain diatoms are frequently observed. The diverse range of mixotrophic strategies utilized in this region speaks to its overall importance. Mixotrophy provides multiple pathways to obtaining essential nutrients and energy in a single cell, better-enabling organisms to withstand the NGA's environmental variability. As observed in this study, there can be large changes in nutrient concentrations, temperature, salinity, and PAR over short spatial and temporal scales, even in summer months. These conditions impact organisms of different sizes and ecological niches differently. The presence of mixotrophy across these groups helps communities respond to environmental drivers based on their particular needs, in turn increasing ecosystem stability and resilience.

Cell size is an important dictator of community structure in the NGA as was observed in our principal component analysis (Fig. 13). Cell size clustered organisms better than taxonomic group, with four distinct clusters being formed: Synechococcus, cells <5 µm, cells 5-10 µm, and cells 10-20 µm. Organisms in the 10-20 µm range were dominated by diatoms and clustered with lower temperatures, indicating relationships among cell size, temperature, and community composition. In future climate regimes, warmer ocean temperatures and increased stratification may lead to a decrease in grazing pressure from micro and mesozooplankton, decreased diatom

abundance, and increased Synechococcus prey concentrations (Finkel et al. 2007; Schmidt et al. 2020). These conditions will likely favor small-celled mixotrophs (Stoecker et al. 2017), a hypothesis that is supported by mixotrophic cells dominating in summer conditions (Chan et al. 2009).

Since the discovery of grazing by protists and the importance of mixotrophy by small-celled phytoflagellates understanding their role as grazers has been a priority of researchers and modelers (Andersen et al. 2015; Sherr and Sherr 2002). Previous studies have shown that phytoflagellates consume most of the cyanobacteria production, with cyanobacteria accumulation only persisting in summer months (Figueiras et al. 2020; Li et al. 2020; Sanders et al. 2000). Grazing by nanoflagellate organisms is a key link in lower trophic food webs and will continue to be important as increased temperatures support small-cells dominance (Agirbas et al. 2015; Capuzzo et al. 2017).

3. Modeling Mixotrophy in the NGA

Modeling efforts in the NGA are working to incorporate mixotrophy into the NGA-adapted NEMURO model used for the LTER site (Fiechter et al. 2011; Kishi et al. 2007). This effort is currently aimed at incorporating large-celled mixotrophy occurring in the ciliate and dinoflagellate communities. The increased understanding of mixotrophy we have gained through this study highlights the importance of small cell (<20 μm) mixotrophs in this region and the need to account for them in modeling efforts as well. The incorporation of mixotrophy into basic food web models highlights how mixotrophy can increase both ecosystem stability, by increasing pathways to nutrients and energy, and productivity, by increasing grazing on small cells and energy capture through photosynthesis (Fig. 15). By combining community composition data,

grazing rates, and relationships between ingestion and environmental conditions, future models of the region can be parameterized based in part on NGA-specific mixotrophy data. This combined modeling and experimental approach will better inform our understanding of the widescale implications of mixotrophy in this system.

Notes on Scale and Future Methodology

Freshwater inputs, eddy formation, the Alaska Coastal Current, and the NGA's bathymetry create a region with a wide array of physical and chemical environments changing on short spatial scales. This complex station-to-station variability make it challenging to group stations and highlights the need for larger sample sizes when examining ingestion in this manner. A study similar to our ambient feeding measurements using flow cytometry or stable isotope probing techniques to examine mixotrophy by nanoflagellates would allow for increased sample sizes, replicates, and potentially broader sampling plans (Anderson et al. 2017, Frias-Lopez et al. 2009).

With our methods for the deckboard incubation experiments it was not possible to differentiate *Synechococcus* that had been ingested before incubation and the cultured *Synechococcus* that was added to experiment bottles, making it hard to separate station-station variability in ambient feeding from experimental responses. We also did not see a change in ingestion for our DIN or PAR experiments for either taxonomic group. If the mixotrophic strategy being employed was either a nutrient acquisition strategy - as we suspect for the nanoflagellates - or an energy acquisition strategy - as we suspect of the dinoflagellates and cryptophytes - we would have expected to see a decrease in ingestion in at least one of these sets of experiments. It could be that the relatively short (4h) incubation period was not long enough

for the organisms to acclimate to the new environmental conditions, particularly within the light experiments. Methods that are less microscopy depended could allow for increased replicates at each treatment level or destructive sampling over a longer incubation period, helping to untangle the background variability from the functional responses.

Increased sample sizes would also allow for the utilization of the kinds of statistical modeling attempted in this study. Given that there seem to be multiple factors influencing feeding by phytoflagellates, statistical modeling approaches would allow examination of independent influences on the patterns observed and provide a deeper understanding of the relationships between the physicochemical environment and feeding responses (Li et al. 2020). Instead, in this case, we relied on the inferences that can be gained from looking at responses across individual factors. Our goal was to gain an initial understanding of small-celled mixotrophy in this region, and to consider the implications for ecosystem structure and resilience. Given that we now know mixotrophy in the NGA is a common strategy utilized by a large fraction of the community, future studies should focus on using methodology that would support larger sample sizes with higher spatial resolution and increased replicates to continue to explore the connection between mixotrophic behavior and the physico-chemical environment.

Tables

Table 1. Station names, sampling date, ambient levels of salinity (psu), temperature (° C), *Synechococcus* (cells/ml), nitrate (μM), and phosphate (μM) concentrations for all stations sampled. Groups enumerated correspond to the taxonomic groups enumerated for ingestion at that station, N = nanoflagellate, D = dinoflagellate, C = cryptophyte. The photosynthetically active radiation (PAR, mol photons m^{-2}) is the PAR dose received over the 16h period prior to sample collection. Asterisks (*) indicate stations where DIN and PAR gradient experiments were conducted; double asterisks (**) indicate stations where prey addition experiments were also conducted.

Station	Date	Groups Enumerated	Salinity	Temp	*Syn.*	Nitrate	Phosphate	PAR
PWS 2*	6/30/19	N, D	28.76	14.65	3.42e4	0.07	0.12	9.65
MID 5*	7/2/19	N	30.57	13.88	1.13e5	0.22	0.26	2.98
PL 1	7/4/19	N	25.61	17.65	2.26e5	1.29	0.36	2.66
PL 2	7/4/19	N	23.24	15.07	1.07e5	0.88	0.14	1.33
PL 4	7/5/19	N	17.42	15.56	1.41e4	0.11	0.14	2.76
PL 5	7/5/19	N, D	28.51	15.73	2.20e5	0.02	0.23	11.05
PL 7	7/6/19	N	30.72	12.37	3.65e5	2.49	0.14	0.52
PL 8	7/6/19	N	30.86	11.91	2.94e5	0.30	0.35	0.65
PL 9	7/7/19	N, D	30.22	14.21	1.09e5	0.24	0.28	2.24
PL 10	7/7/19	N, D	30.48	12.36	2.94e5	0.10	0.10	2.67
GAK 15**	7/9/19	N, D	32.26	14.39	2.22e4	0.96	0.39	3.67
GAK 9**	7/10/19	N	32.12	12.68	4.80e5	1.43	0.41	2.25
GAK 5**	7/12/19	N	31.23	14.60	2.20e5	0.32	0.40	1.73
KOD 3**	7/15/19	N	31.98	11.63	2.95e4	0.48	0.43	4.68
KOD 8**	7/16/19	N	32.14	13.07	5.43e5	0.46	0.41	3.35
PWS 1	9/12/19	N, D, C	22.53	13.60	2.08e5	0.09	0.00	1.12
PWS 2	9/12/19	N, D, C	26.41	13.98	1.70e5	0.06	0.05	1.58
PWS 3	9/13/19	N, D, C	25.96	13.91	2.07e5	0.09	0.02	0.42
MID 2	9/14/19	N, D, C	30.05	14.03	9.14e4	0.01	0.15	1.06
MID 5	9/15/19	N, D	27.32	14.71	3.21e4	0.02	0.03	1.30
GAK 1	9/16/19	N, D, C	26.34	13.53	4.28e4	0.10	0.09	1.14
GAK 5	9/17/19	N, C	30.83	11.98	6.35e3	0.43	0.28	0.55
GAK 9	9/19/19	N, D, C	31.96	11.81	1.22e5	2.72	0.53	0.75
KOD 3	9/22/19	N, C	30.72	11.24	6.44e4	4.99	0.64	2.08
KOD 5	9/22/19	N, D, C	31.15	11.26	1.03e5	5.54	0.67	2.80

Table 2. Variable loadings and proportion of variance explained for the first three components of PCA examining environmental factors at stations sampled during summer and fall 2019.

	PC1	PC2	PC3
Proportion of Variance	0.372	0.168	0.155
Cumulative Proportion	0.372	0.540	0.696
Variable:			
Salinity	-0.470	0.126	0.339
Temperature	0.488	0.205	0.012
Synechococcus	-0.128	-0.133	0.848
Nitrate	-0.486	-0.012	-0.365
Phosphate	-0.527	0.272	-0.136
Ammonium	-0.008	0.455	0.008
PAR	0.103	0.802	0.121

Table 3. Variable loadings and proportion of variance explained for the first three components of PCA examining community composition of samples taken in summer and fall 2019 analyzed by taxon.

	PC1	PC2	PC3
Proportion of Variance	0.325	0.212	0.173
Cumulative Proportion	0.325	0.536	0.701
Variable:			
Synechococcus	0.226	-0.430	0.046
Misc. Autotrophic Flagellate	-0.375	-0.446	-0.424
Picoeukaryote	-0.271	-0.444	0.559
Cryptophyte	-0.282	0.184	0.661
Nanoflagellate	-0.460	0.204	0.010
Dinoflagellate	-0.529	-0.301	-0.177
Diatom	-0.405	0.503	-0.195

Table 4. Variable loadings and proportion of variance explained for the first three components of PCA examining community composition of samples taken in summer and fall 2019 analyzed by size class.

	PC1	PC2	PC3
Proportion of Variance	0.341	0.201	0.183
Cumulative Proportion	0.341	0.542	0.723
Variable:			
Synechococcus	-0.300	0.538	-0.009
0-2.5	0.256	0.676	-0.043
2.5-5	0.155	0.301	-0.719
5-10	0.112	-0.402	-0.655
10-15	0.639	0.017	0.113
15-20	0.633	-0.040	0.196

Figures

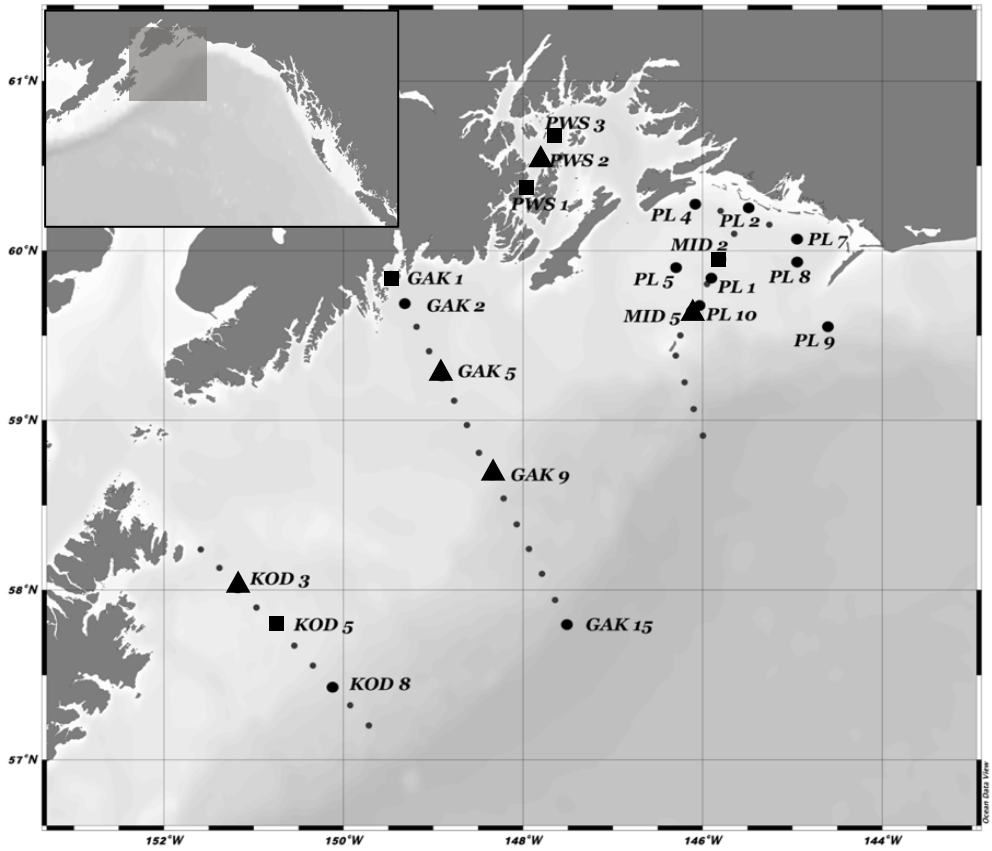

Figure 1. Stations sampled during the summer and fall 2019 LTER cruises. Labels denote stations where experiments were conducted, or where samples were taken for ambient feeding analysis and community composition determination. Large circles represent stations sampled in summer only, squares represent stations sampled in fall only, and triangles represent stations sampled in both summer and fall. Stations were sampled along the Kodiak Line (KOD), Seward Line (GAK), Middleton Island Line (MID), in Prince William Sound (PWS), and in the Copper River Plume Study Area (PL). Inset shows sampling area in the larger context of the southern Alaska coastline.

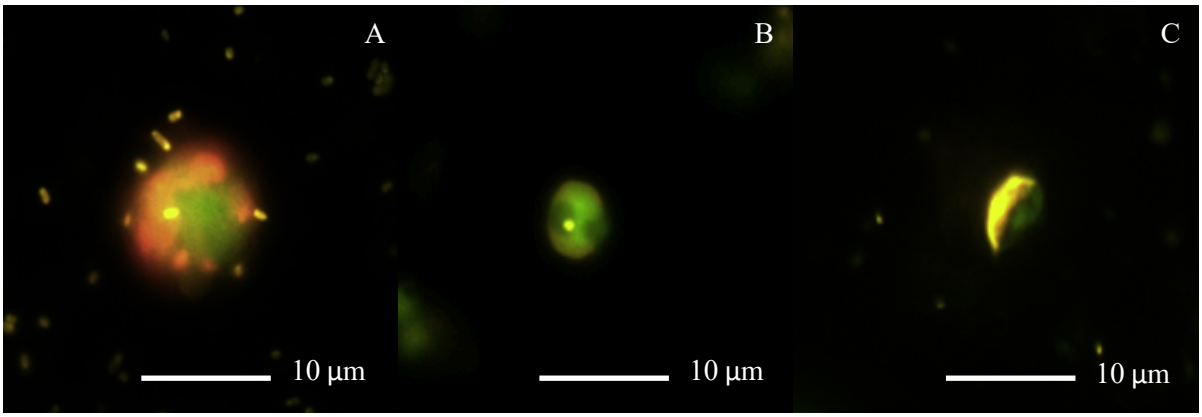

Figure 2. Images of a mixotrophic dinoflagellate (A), nanoflagellate (B), and cryptophyte (C) under 1000x epifluorescence illumination. Within the dinoflagellate cell (A) and nanoflagellate cell (B) am ingested *Synechococcus* can be observed. Red autofluorescence of chloroplasts allowed for determination of inherent photosynthetic ability and yellow autofluorescence of *Synechococcus* was used to observe ingestion.

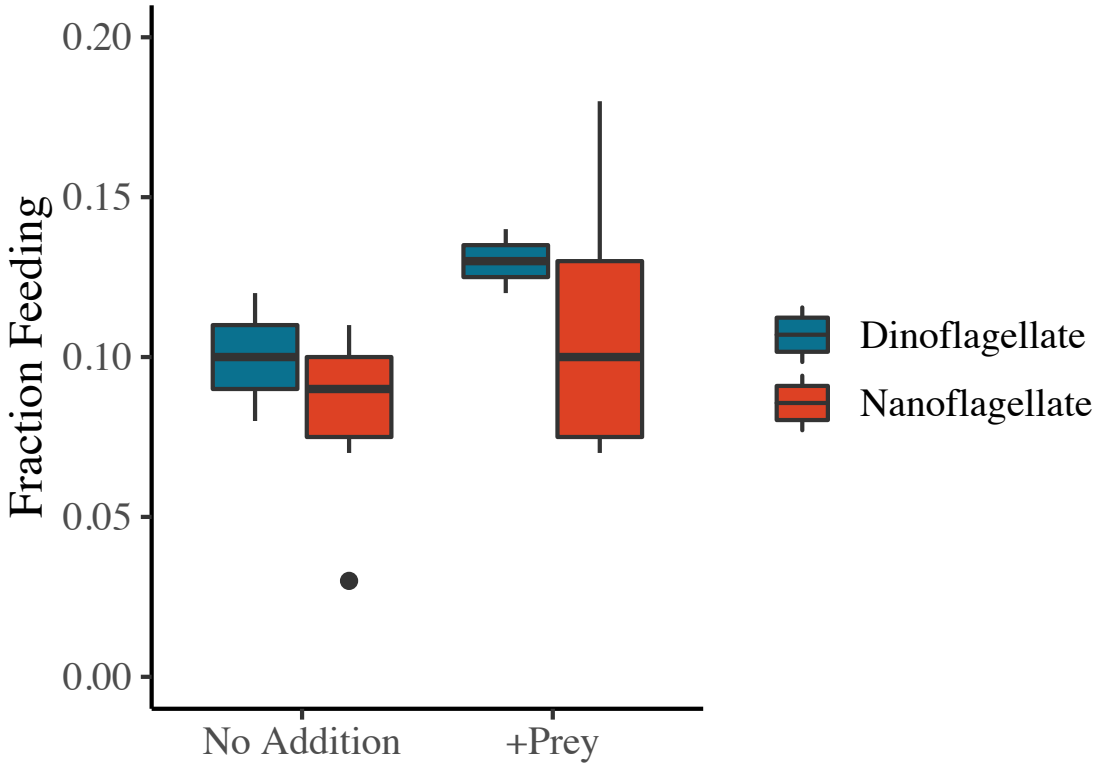

Figure 3. Box plot displaying fraction feeding for nanoflagellates (red) and dinoflagellates (blue) with and without added cultured *Synechococcus* cells. Samples were screened to 50% ambient PAR and incubated on deck for 4h with no nutrient addition. Two bottles were incubated with added prey ($1x10^6$-$5x10^6$ cells/ml) and two without for each set of experiment (n=14). Bottom, middle and top of boxes denote the first quartile, median, and third quartile respectively, with the whiskers representing the 10th and 90th percentile.

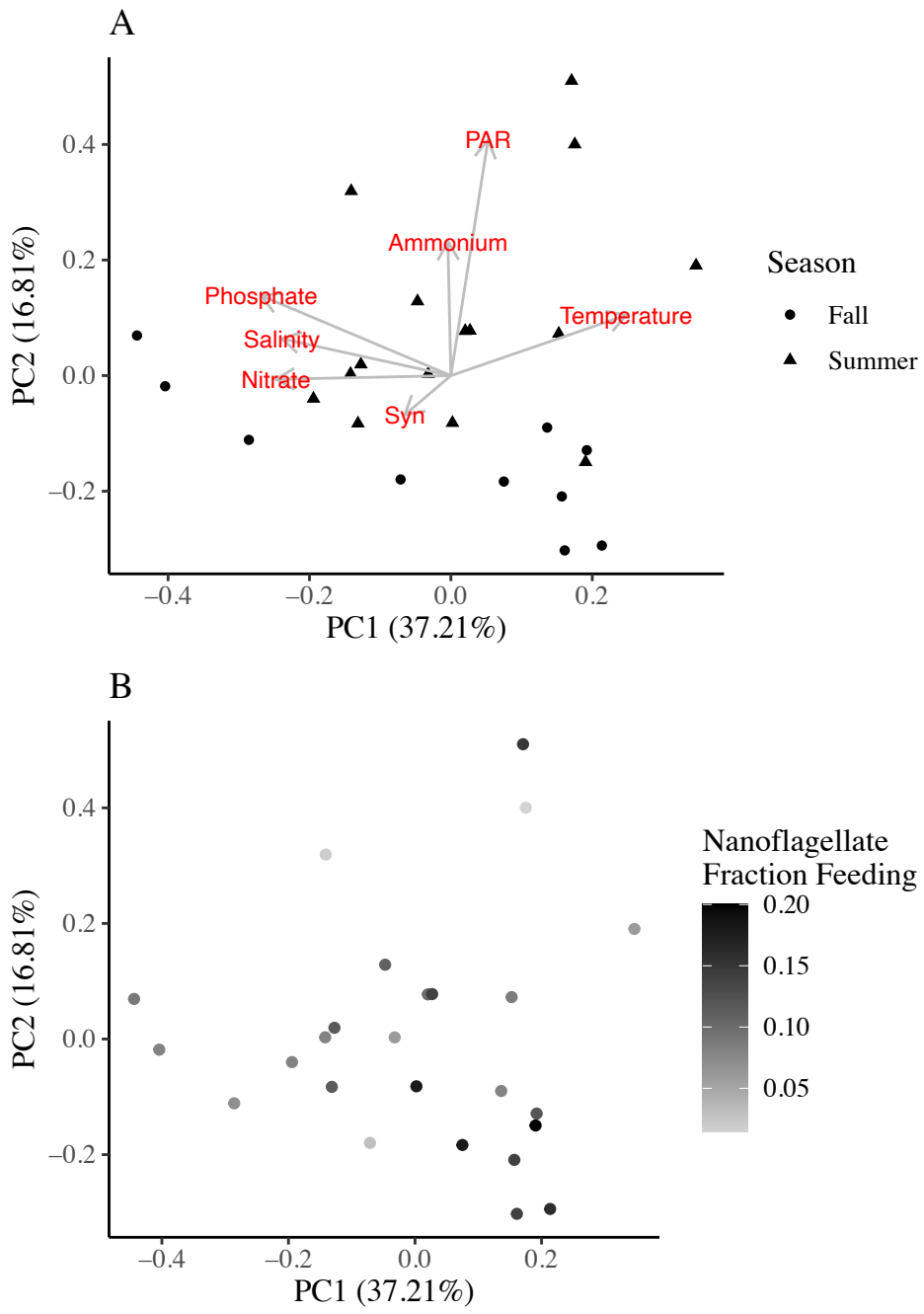

Figure 4. Principal component analysis on environmental factors in the NGA by season (A) with fraction feeding of the nanoflagellate community overlain (B). Arrows show the loadings for each variable; axes show % of total variance explained by PC1 and PC2. Darker circles in (B) correspond to a higher fraction of nanoflagellate feeding.

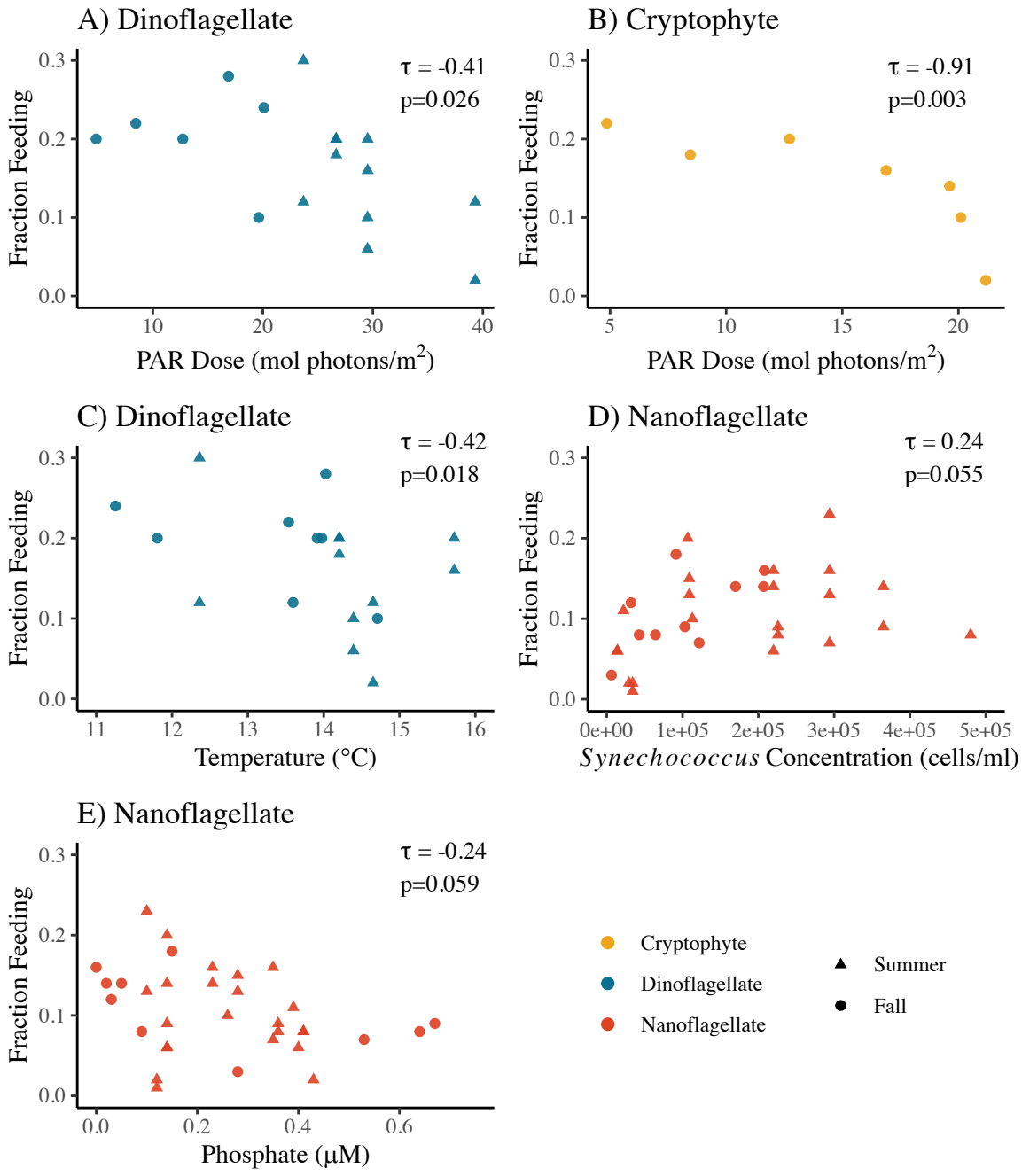

Figure 5. Significant (α =0.1) correlations between ingestion (fraction feeding) and environmental variables for A) dinoflagellates and B) cryptophytes versus 24-h light history; C) dinoflagellates versus temperature; D) nanoflagellates versus *Synechococcus* concentration; E) nanoflagellates versus phosphate concentration. Correlation coefficients (Kendall's tau) and p-values are shown on each plot. Both summer (triangle) and fall (circle) data are included in this analysis. Color indicates the mixotroph taxonomic group: cryptophyte (yellow), dinoflagellate (blue) or nanoflagellate (red).

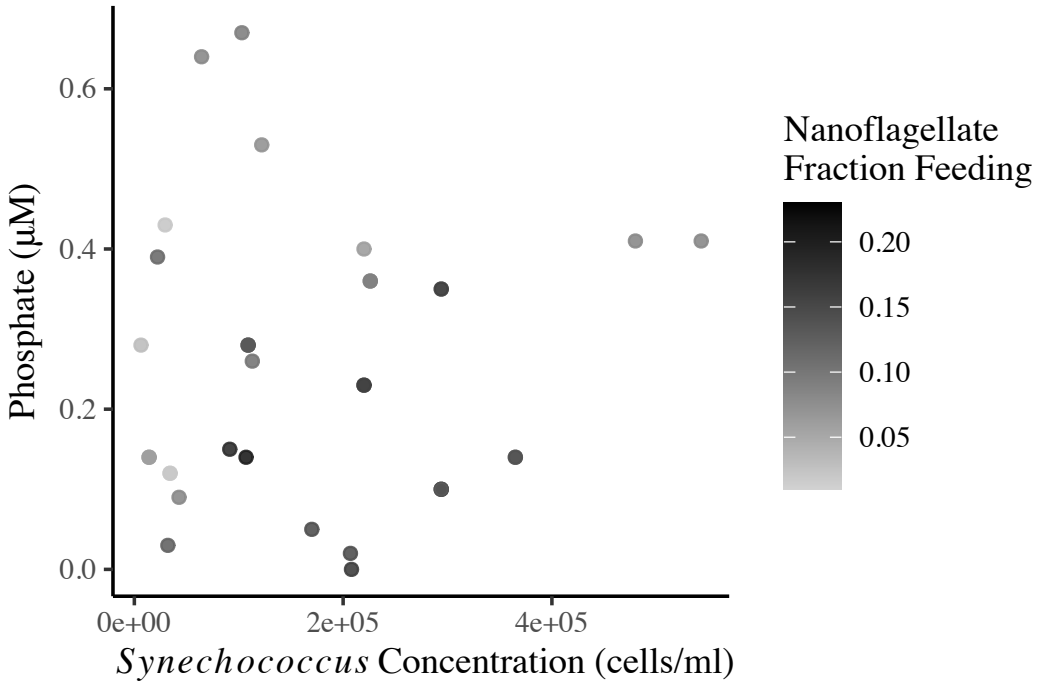

Figure 6. Ambient fraction feeding by the nanoflagellate community as a function of *Synechococcus* and phosphate concentrations. Greyscale corresponds to the fraction of the community feeding with darker points corresponding to stations with higher ingestion rates. Nutrient and *Synechococcus* concentration estimates came from the same Niskin bottles as the samples used to determine fraction feeding. Both summer and fall data are included.

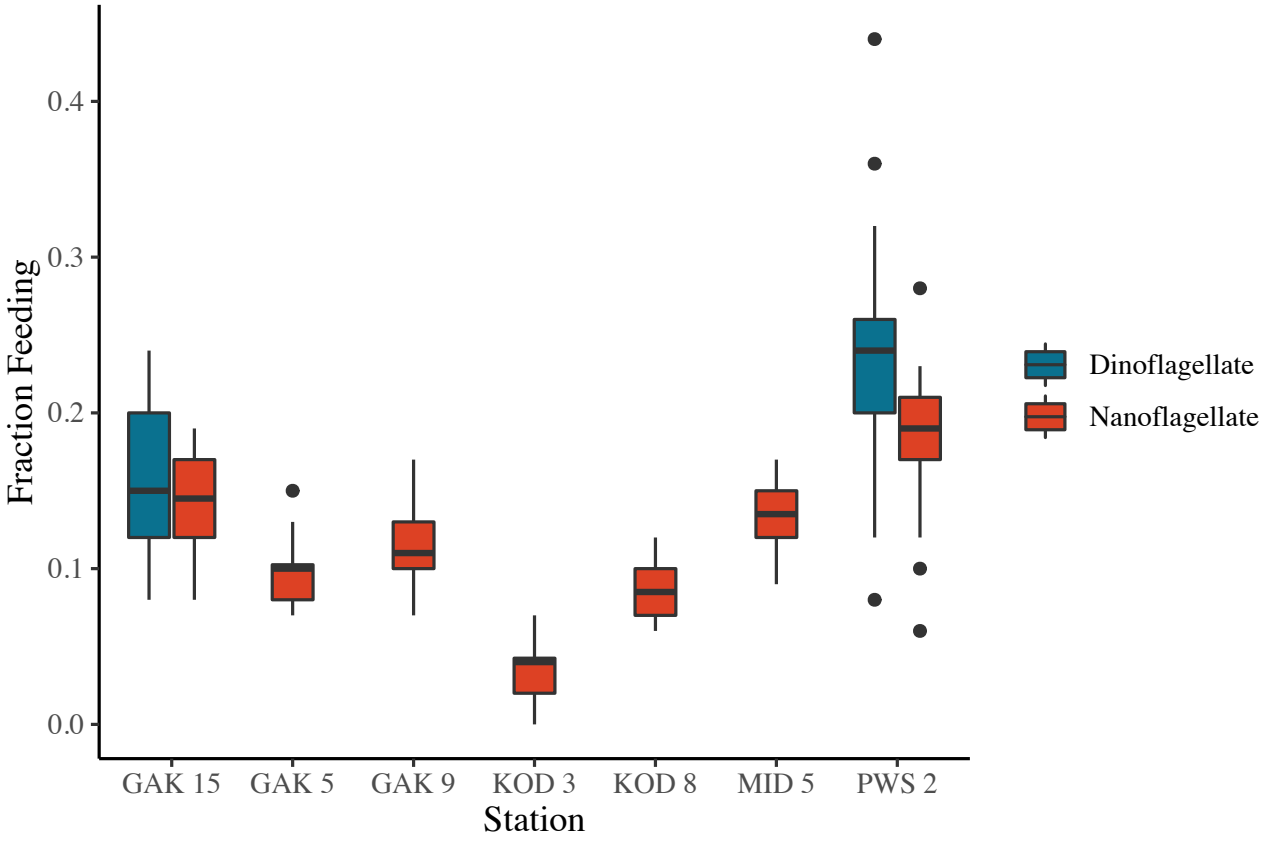

Figure 7. Boxplot of fraction feeding for experiments conducted in summer 2019. All experiments from a given station were averaged regardless of treatment (n=22-64). All samples were incubated for 4h. Dinoflagellates (blue) were only enumerated at GAK 15 and PWS 2; nanoflagellates (red) were enumerated at every station. The boxes represent the first quartile, median, and third quartile, with whiskers extending to the 10th and 90th percentiles; any outliers are shown as points above or below the whiskers.

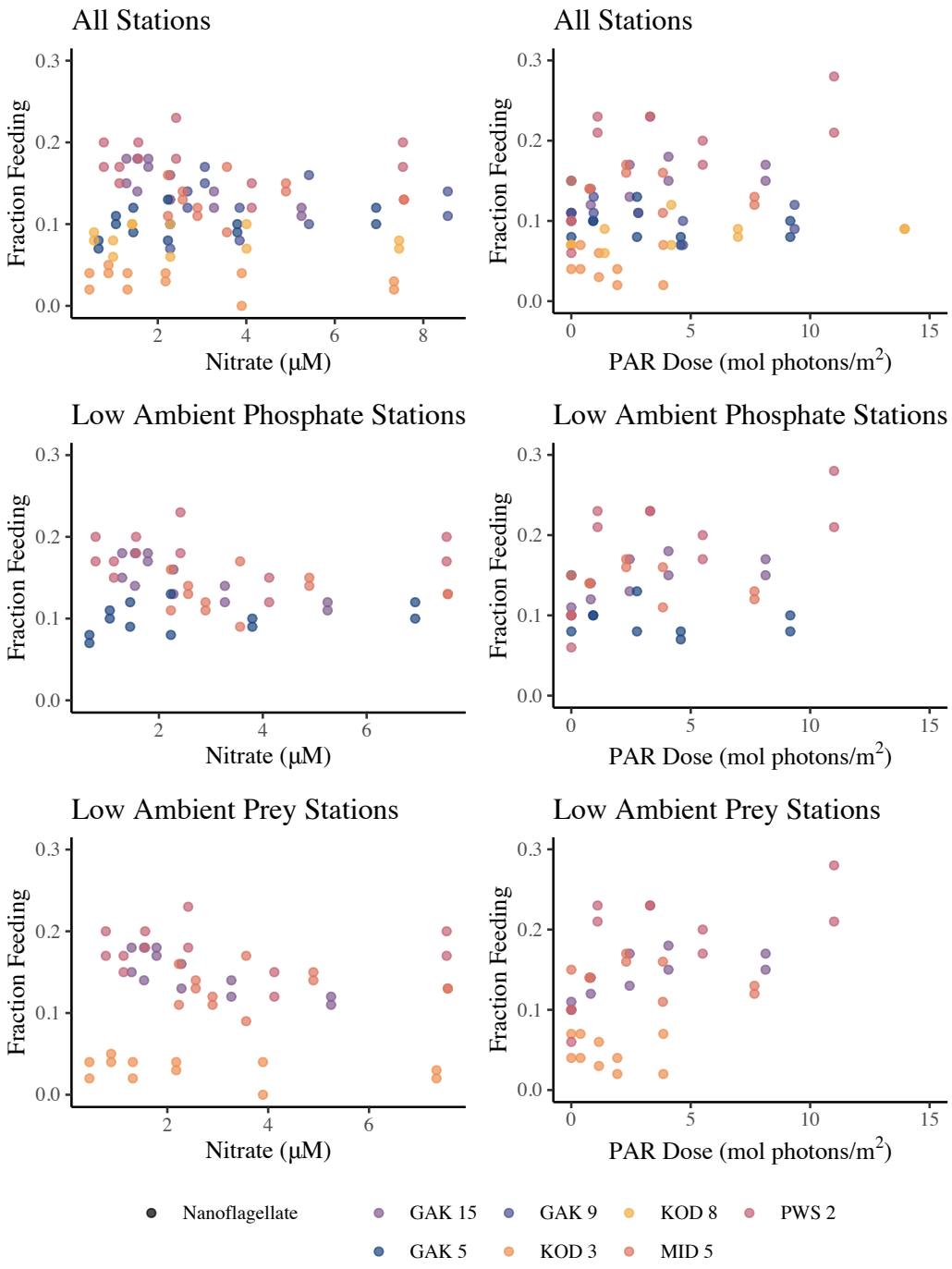

Figure 8. Fraction feeding for the nanoflagellate community in response to gradients of PAR dose and DIN during summer experiments. Low ambient phosphate stations were determined to have <0.4 µM phosphate and low ambient prey stations were classified as having <2x10^5 cells/ml *Synechococcus* prior to prey addition. Darker points represent stations were replicate samples had the same fraction feeding, lines correspond to standard error between replicates (n=2). The PAR values represent the total PAR received during 4 h deck incubations. All samples received additions of cultured *Synechococcus.*

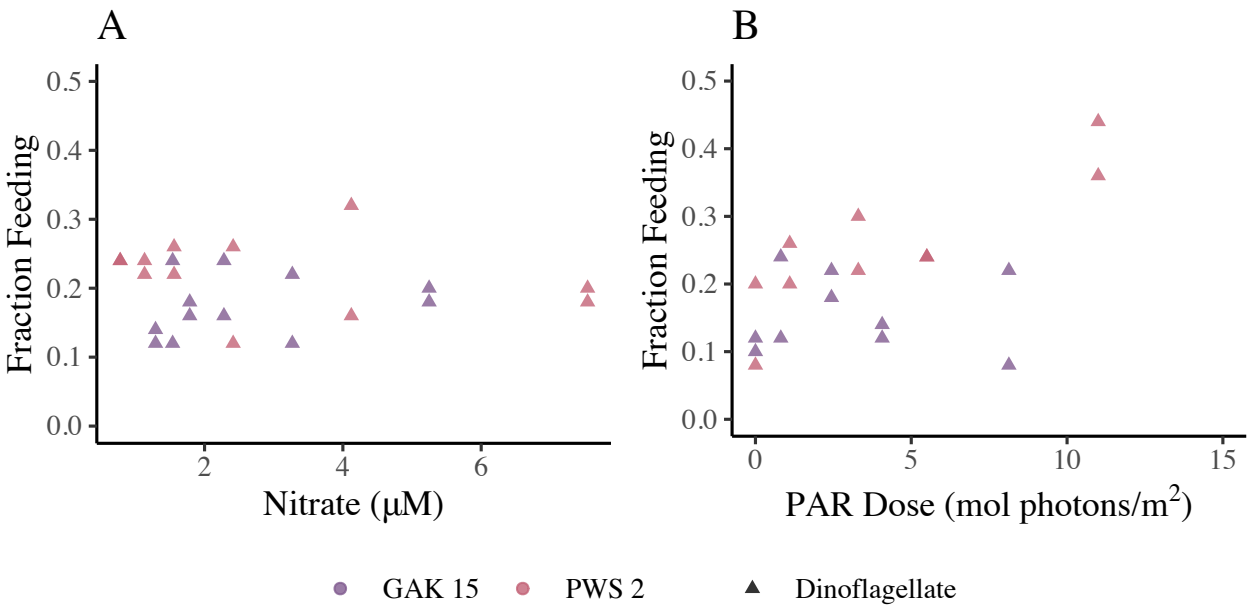

Figure 9. Fraction feeding for the dinoflagellate community in response to gradients of DIN and PAR during summer experiments. A) fraction feeding in response to increased Nitrate concentration; B) fraction feeding in response to PAR Dose. Darker points represent stations were replicate samples had the same fraction feeding. All stations sampled were determined to be low phosphate (<0.4 µM) and low *Synechococcus* (<2x10^5 cells/ml). The PAR values represent the total PAR received during 4 h deck incubations. All samples received additions of cultured *Synechococcus.*

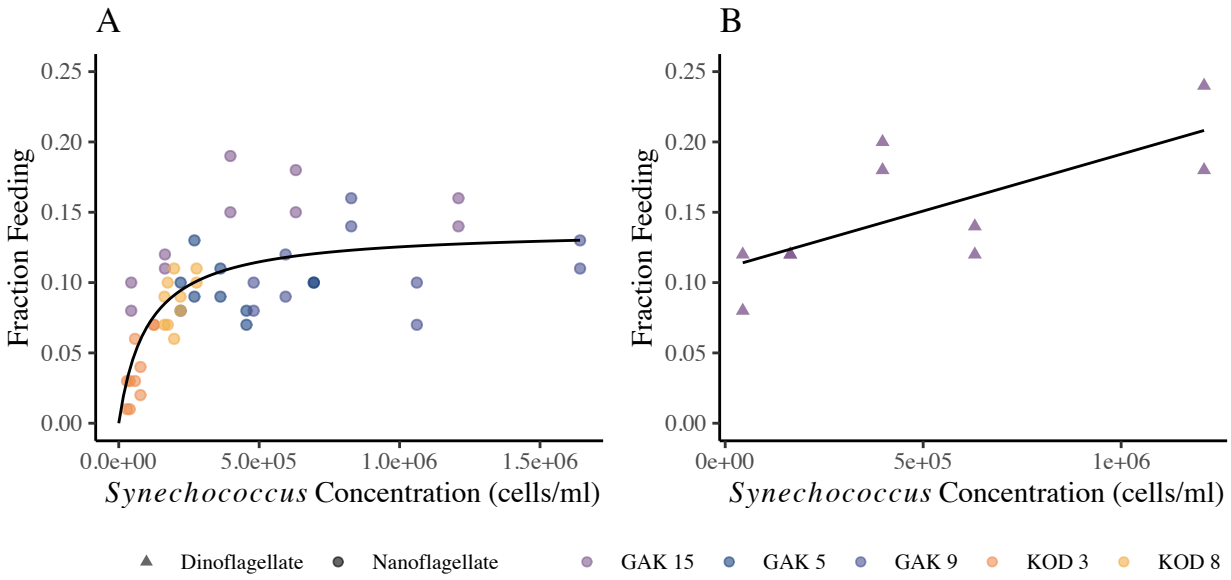

Figure 10. Feeding responses to increased *Synechococcus* cell concentrations during summer experiments. A) the nanoflagellate feeding response fit with a Michaelis-Menten response curve (residual standard error=0.029; B) the dinoflagellate feeding response fit using a glm (fraction feeding ~ *Synechococcus* concentration, p=0.017, 8 df, R^2=0.53). These data represent all stations where prey concentration experiments were conducted and there was a mixotroph community of sufficient abundance to enumerate (only GAK 15 for the dinoflagellate community). All samples were screened to 50% ambient PAR, deck incubated for 4 h and received gradients in cultured *Synechococcus.* Darker points represent stations where replicate samples had the same fraction feeding, color corresponds to station.

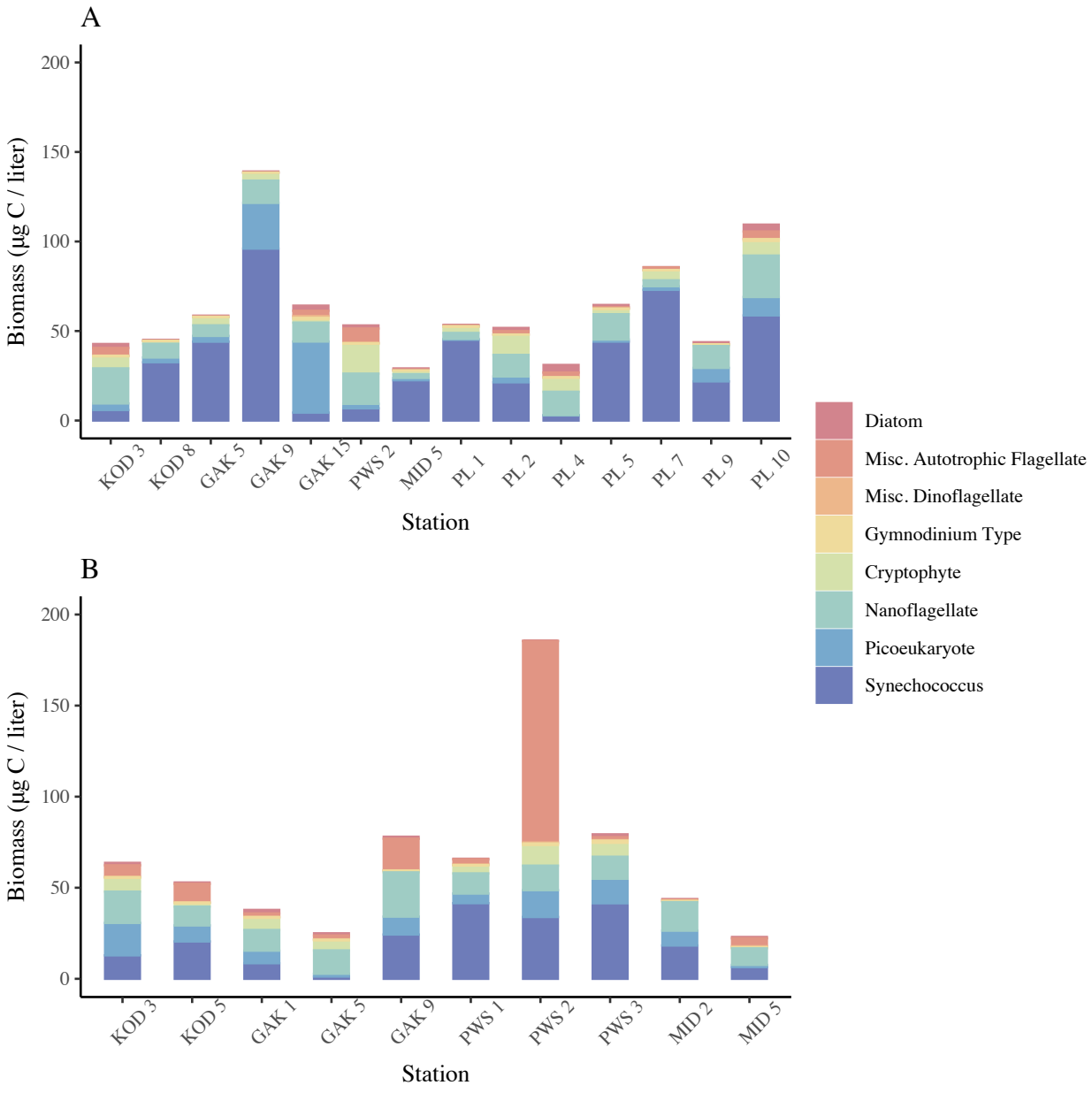

Figure 11. Biomass of <20 µm photosynthetic community separated by taxonomic group for each station sampled in A) summer and B) fall. Gymnodinium-types and Cryptophytes are shown separately from Misc. Dinoflagellates and Nanoflagellates since the former were enumerated independently for fraction feeding analysis.

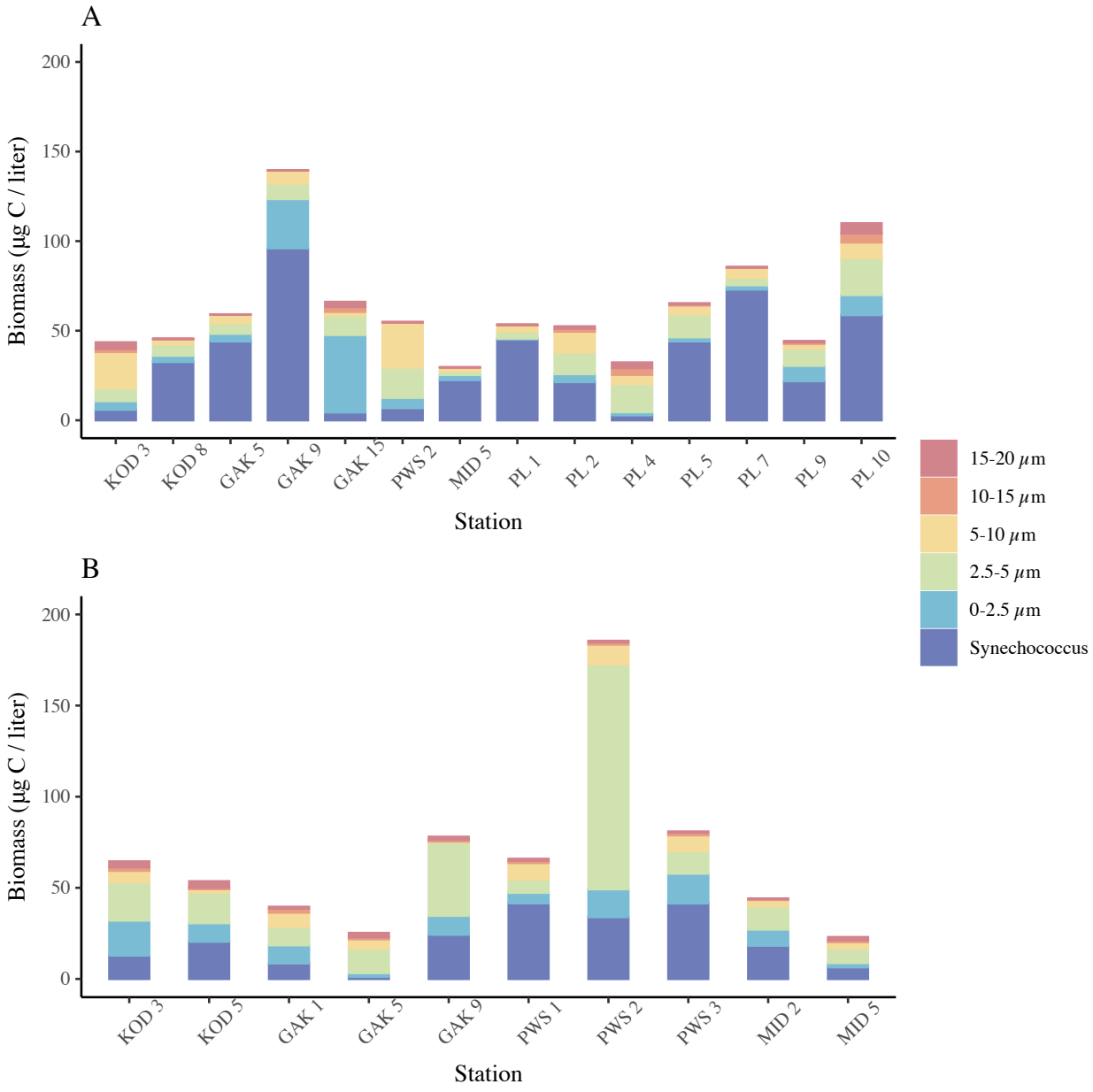

Figure 12. Biomass of <20 µm photosynthetic eukaryote community separated by size class (with *Synechococcus* shown separately) for each station sampled in A) summer and B) fall.

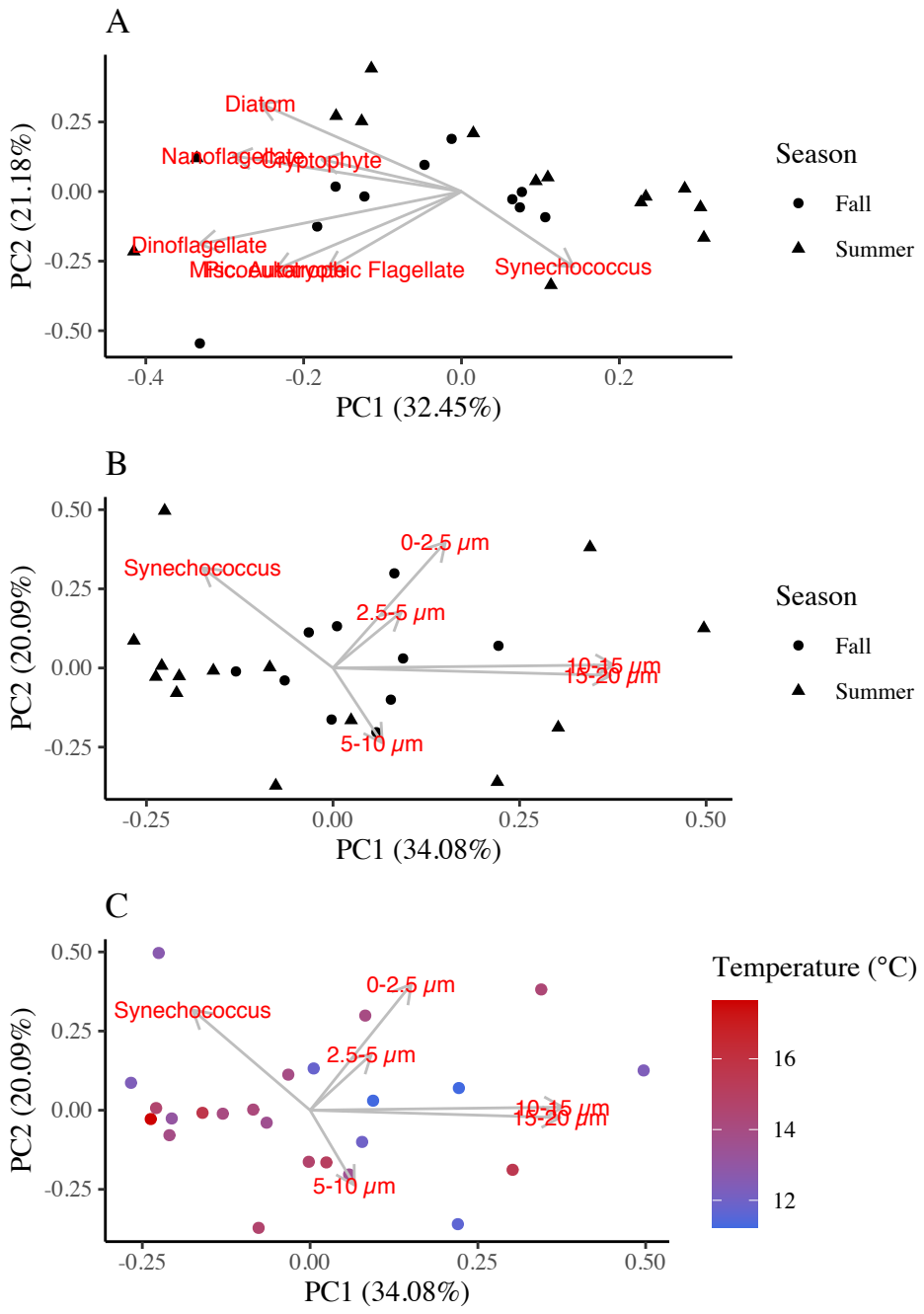

Figure 13. Principal component analysis for <20 µm community by A) taxon and B, C) size class. Vectors show taxon or size class loadings, with axes showing % of total variance explained by PC1 and PC2. Shapes indicate season (A, B), color in C) corresponds to temperature.

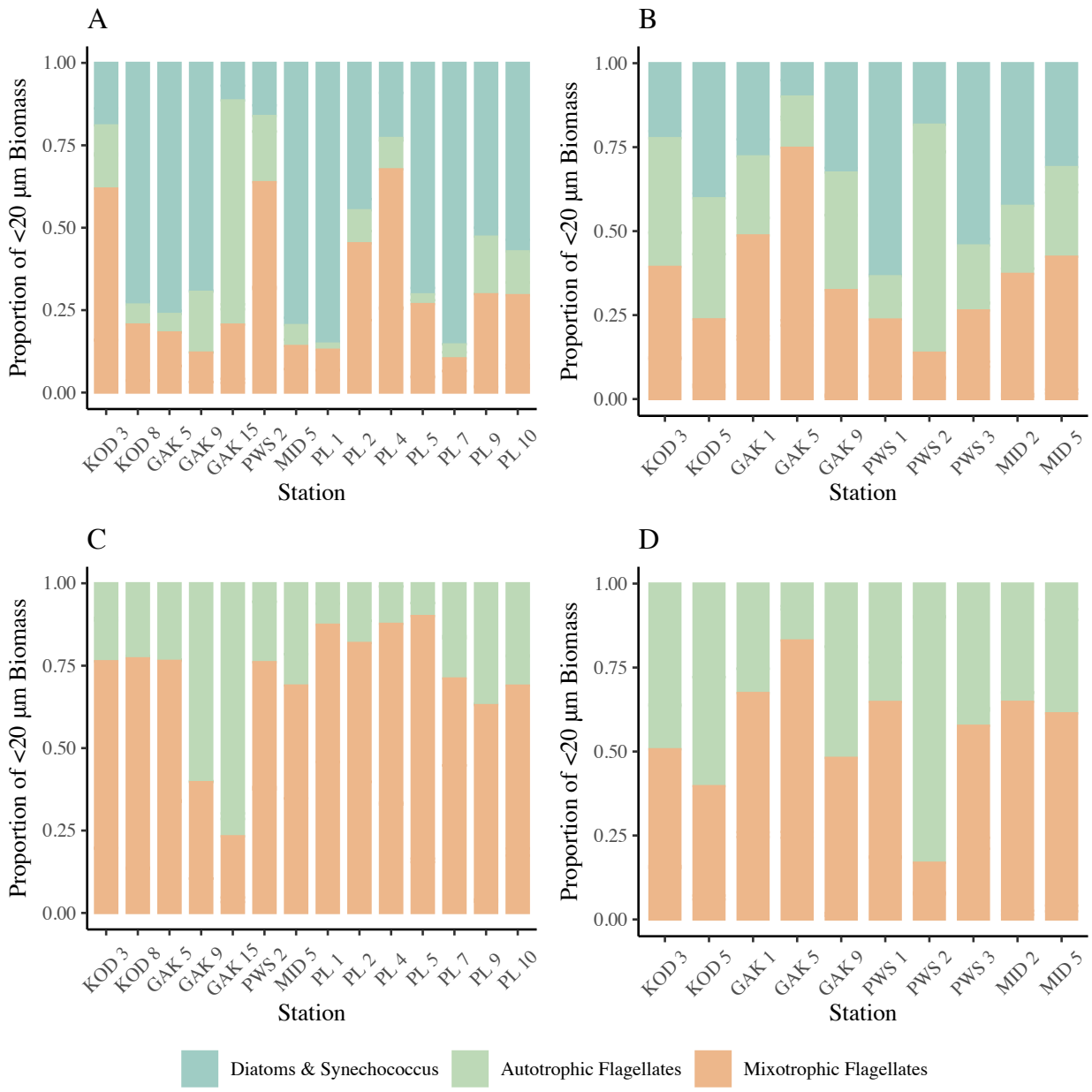

Figure 14. Mixotrophic flagellates as a proportion of <20 µm photosynthetic community biomass (µgC/L) observed to be mixotrophic during summer (A) and fall (B). Mixotrophic organisms were classified by direct observation of ingested *Synechococcus* prey in this study and include the groups enumerated for fraction feeding analysis. Mixotrophic flagellates as a proportion of total <20 µm phytoflagellates shown for summer (C) and fall (D).

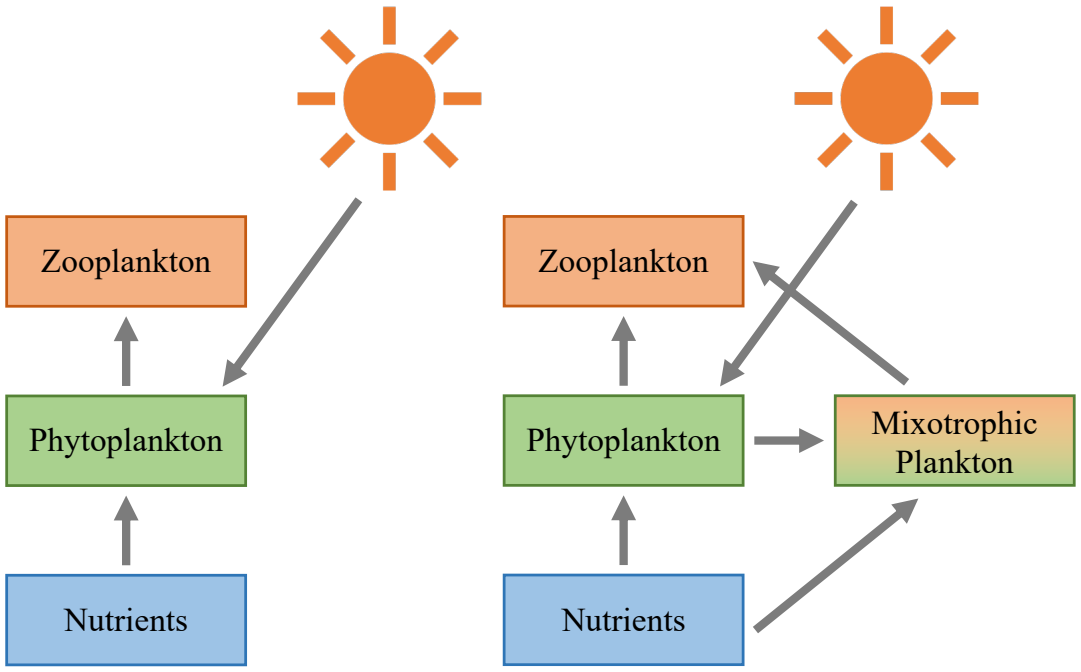

Figure 15. Schematic diagrams of basic microplankton food webs without mixotrophy incorporated (left) and with mixotrophy incorporated (right). The incorporation of mixotrophy as a pathway for nutrients and energy shows how mixotrophic organisms contribute to ecosystem stability and productivity.

Literature Cited

Agirbas, E., Martinez-Vicente, V., Brewin, R. J. W., Racault, M.-F., Airs, R. L., & Llewellyn, C. A. (2015). Temporal changes in total and size-fractioned chlorophyll-a in surface waters of three provinces in the Atlantic Ocean (September to November) between 2003 and 2010. *Journal of Marine Systems*, *150*, 56–65. https://doi.org/10.1016/j.jmarsys.2015.05.008

Agirbas et al. - 2015—Temporal changes in total and size-fractioned chlo.pdf. (n.d.).

Aguilar-Islas, A. M., Séguret, M. J. M., Rember, R., Buck, K. N., Proctor, P., Mordy, C. W., & Kachel, N. B. (2016). Temporal variability of reactive iron over the Gulf of Alaska shelf. *Deep Sea Research Part II: Topical Studies in Oceanography*, *132*, 90–106. https://doi.org/10.1016/j.dsr2.2015.05.004

Aguilar-Islas, A. M., Wu, J., Rember, R., Johansen, A. M., & Shank, L. M. (2010). Dissolution of aerosol-derived iron in seawater: Leach solution chemistry, aerosol type, and colloidal iron fraction. *Marine Chemistry*, *120*(1–4), 25–33. https://doi.org/10.1016/j.marchem.2009.01.011

Andersen, K. H., Aksnes, D. L., Berge, T., Fiksen, Ø., & Visser, A. (2015). Modelling emergent trophic strategies in plankton. *Journal of Plankton Research*, *37*(5), 862–868. https://doi.org/10.1093/plankt/fbv054

Anderson, R., Charvet, S., & Hansen, P. J. (2018). Mixotrophy in Chlorophytes and Haptophytes—Effect of Irradiance, Macronutrient, Micronutrient and Vitamin Limitation. *Frontiers in Microbiology*, *9*, 1704. https://doi.org/10.3389/fmicb.2018.01704

Anderson, R., Jürgens, K., & Hansen, P. J. (2017). Mixotrophic Phytoflagellate Bacterivory Field Measurements Strongly Biased by Standard Approaches: A Case Study. *Frontiers in Microbiology*, *8*, 1398. https://doi.org/10.3389/fmicb.2017.01398

Arenovski, A. L., Lim, E. L., & Caron, D. A. (1995). Mixotrophic nanoplankton in oligotrophic surface waters of the Sargasso Sea may employ phagotrophy to obtain major nutrients. *Journal of Plankton Research*, *17*(4), 801–820. https://doi.org/10.1093/plankt/17.4.801

Beisner, B. E., Grossart, H.-P., & Gasol, J. M. (2019). A guide to methods for estimating phago-mixotrophy in nanophytoplankton. *Journal of Plankton Research*, *41*(2), 77–89. https://doi.org/10.1093/plankt/fbz008

Boyd, P. W., Law, C. S., Wong, C. S., Nojiri, Y., Tsuda, A., Levasseur, M., Takeda, S., Rivkin, R., Harrison, P. J., Strzepek, R., Gower, J., McKay, R. M., Abraham, E., Arychuk, M., Barwell-Clarke, J., Crawford, W., Crawford, D., Hale, M., Harada, K., … Yoshimura, T. (2004). The decline and fate of an iron-induced subarctic phytoplankton bloom. *Nature*, *428*(6982), 549–553. https://doi.org/10.1038/nature02437

Capuzzo, E., Lynam, C. P., Barry, J., Stephens, D., Forster, R. M., Greenwood, N., McQuatters-Gollop, A., Silva, T., van Leeuwen, S. M., & Engelhard, G. H. (2018). A decline in primary production in the North Sea over 25 years, associated with reductions in zooplankton abundance

and fish stock recruitment. *Global Change Biology*, *24*(1), e352–e364. https://doi.org/10.1111/gcb.13916

Capuzzo et al. - 2018—A decline in primary production in the North Sea o.pdf. (n.d.).

Cavole, L., Demko, A., Diner, R., Giddings, A., Koester, I., Pagniello, C., Paulsen, M.-L., Ramirez-Valdez, A., Schwenck, S., Yen, N., Zill, M., & Franks, P. (2016). Biological Impacts of the 2013–2015 Warm-Water Anomaly in the Northeast Pacific: Winners, Losers, and the Future. *Oceanography*, *29*(2). https://doi.org/10.5670/oceanog.2016.32

Chan, Y.-F., Chiang, K.-P., Ku, Y., & Gong, G.-C. (2019). Abiotic and Biotic Factors Affecting the Ingestion Rates of Mixotrophic Nanoflagellates (Haptophyta). *Microbial Ecology*, *77*(3), 607–615. https://doi.org/10.1007/s00248-018-1249-2

Chan, Y.-F., Tsai, A.-Y., Chiang, K.-P., & Hsieh, C. (2009). Pigmented Nanoflagellates Grazing on Synechococcus: Seasonal Variations and Effect of Flagellate Size in the Coastal Ecosystem of Subtropical Western Pacific. *Microbial Ecology*, *58*(3), 548–557. https://doi.org/10.1007/s00248-009-9569-x

Duhamel, S., Kim, E., Sprung, B., & Anderson, O. R. (2019). Small pigmented eukaryotes play a major role in carbon cycling in the P-depleted western subtropical North Atlantic, which may be supported by mixotrophy. *Limnology and Oceanography*, *64*(6), 2424–2440. https://doi.org/10.1002/lno.11193

Faure, E., Not, F., Benoiston, A.-S., Labadie, K., Bittner, L., & Ayata, S.-D. (2019). Mixotrophic protists display contrasted biogeographies in the global ocean. *The ISME Journal*, *13*(4), 1072–1083. https://doi.org/10.1038/s41396-018-0340-5

Fiechter, J., Broquet, G., Moore, A. M., & Arango, H. G. (2011). A data assimilative, coupled physical–biological model for the Coastal Gulf of Alaska. *Dynamics of Atmospheres and Oceans*, *52*(1–2), 95–118. https://doi.org/10.1016/j.dynatmoce.2011.01.002

Figueiras, F. G., Arbones, B., Castro, C. G., Froján, M., & Teixeira, I. G. (2020). About Pigmented Nanoflagellates and the Importance of Mixotrophy in a Coastal Upwelling System. *Frontiers in Marine Science*, *7*. https://doi.org/10.3389/fmars.2020.00144

Finkel, Z. V., Sebbo, J., Feist-Burkhardt, S., Irwin, A. J., Katz, M. E., Schofield, O. M. E., Young, J. R., & Falkowski, P. G. (2007). A universal driver of macroevolutionary change in the size of marine phytoplankton over the Cenozoic. *Proceedings of the National Academy of Sciences*, *104*(51), 20416–20420. https://doi.org/10.1073/pnas.0709381104

Flynn, K. J., & Mitra, A. (2009). Building the "perfect beast": Modelling mixotrophic plankton. *Journal of Plankton Research*, *31*(9), 965–992. https://doi.org/10.1093/plankt/fbp044

Flynn, Kevin J., Stoecker, D. K., Mitra, A., Raven, J. A., Glibert, P. M., Hansen, P. J., Granéli, E., & Burkholder, J. M. (2013). Misuse of the phytoplankton–zooplankton dichotomy: The need to assign organisms as mixotrophs within plankton functional types. *Journal of Plankton Research*, *35*(1), 3–11. https://doi.org/10.1093/plankt/fbs062

Frias-Lopez, J., Thompson, A., Waldbauer, J., & Chisholm, S. W. (2009). Use of stable isotope-labelled cells to identify active grazers of picocyanobacteria in ocean surface waters. *Environmental Microbiology*, *11*(2), 512–525. https://doi.org/10.1111/j.1462-2920.2008.01793.x

Hansen, P. J. (2011). The Role of Photosynthesis and Food Uptake for the Growth of Marine Mixotrophic Dinoflagellates1: MIXOTROPHY IN MARINE DINOFLAGELLATES. *Journal of Eukaryotic Microbiology*, *58*(3), 203–214. https://doi.org/10.1111/j.1550-7408.2011.00537.x

Hansen, P., & Nielsen, T. (1997). Mixotrophic feeding of Fragilidium subglobosum (Dinophyceae) on three species of Ceratium:effects of prey concentration, prey species and light intensity. *Marine Ecology Progress Series*, *147*, 187–196. https://doi.org/10.3354/meps147187

Heldal, M., Scanlan, D. J., Norland, S., Thingstad, F., & Mann, N. H. (2003). Elemental composition of single cells of various strains of marine *Prochlorococcus* and *Synechococcus* using X-ray microanalysis. *Limnology and Oceanography*, *48*(5), 1732–1743. https://doi.org/10.4319/lo.2003.48.5.1732

Holling, C. S. (1959). Some Characteristics of Simple Types of Predation and Parasitism1. *The Canadian Entomologist*, *91*(7), 385–398. https://doi.org/10.4039/Ent91385-7

Holling, C. S. (1965). The Functional Response of Predators to Prey Density and its Role in Mimicry and Population Regulation. *The Memoirs of the Entomological Society of Canada*, *97*(S45), 5–60. https://doi.org/10.4039/entm9745fv

Hollowed, A. B., Hare, S. R., & Wooster, W. S. (2001). Pacific Basin climate variability and patterns of Northeast Pacific marine fish production. *Progress in Oceanography*, *49*(1–4), 257–282. https://doi.org/10.1016/S0079-6611(01)00026-X

Hutchins, D. A., & Bruland, K. W. (1998). Iron-limited diatom growth and Si:N uptake ratios in a coastal upwelling regime. *Nature*, *393*(6685), 561–564. https://doi.org/10.1038/31203

Jeong, H. J., Lee, K. H., Yoo, Y. D., Kang, N. S., Song, J. Y., Kim, T. H., Seong, K. A., Kim, J. S., & Potvin, E. (2018). Effects of light intensity, temperature, and salinity on the growth and ingestion rates of the red-tide mixotrophic dinoflagellate Paragymnodinium shiwhaense. *Harmful Algae*, *80*, 46–54. https://doi.org/10.1016/j.hal.2018.09.005

Jeong, H. J., Yoo, Y. D., Kim, J. S., Seong, K. A., Kang, N. S., & Kim, T. H. (2010a). Growth, feeding and ecological roles of the mixotrophic and heterotrophic dinoflagellates in marine planktonic food webs. *Ocean Science Journal*, *45*(2), 65–91. https://doi.org/10.1007/s12601-010-0007-2

Jeong, H. J., Yoo, Y. D., Kim, J. S., Seong, K. A., Kang, N. S., & Kim, T. H. (2010b). Growth, feeding and ecological roles of the mixotrophic and heterotrophic dinoflagellates in marine planktonic food webs. *Ocean Science Journal*, *45*(2), 65–91. https://doi.org/10.1007/s12601-010-0007-2

Jeong, H., Park, J., Nho, J., Park, M., Ha, J., Seong, K., Jeng, C., Seong, C., Lee, K., & Yih, W. (2005). Feeding by red-tide dinoflagellates on the cyanobacterium Synechococcus. *Aquatic Microbial Ecology*, *41*, 131–143. https://doi.org/10.3354/ame041131

Jeong, H., Yoo, Y., Park, J., Song, J., Kim, S., Lee, S., Kim, K., & Yih, W. (2005). Feeding by phototrophic red-tide dinoflagellates: Five species newly revealed and six species previously known to be mixotrophic. *Aquatic Microbial Ecology*, *40*, 133–150. https://doi.org/10.3354/ame040133

Kang, H. C., Jeong, H. J., Lim, A. S., Ok, J. H., You, J. H., Park, S. A., Lee, S. Y., & Eom, S. H. (2020). Effects of temperature on the growth and ingestion rates of the newly described mixotrophic dinoflagellate Yihiella yeosuensis and its two optimal prey species. *ALGAE*, *35*(3), 263–275. https://doi.org/10.4490/algae.2020.35.8.20

Kemp, P. F., Cole, J. J., Sherr, B. F., & Sherr, E. B. (2018). *Handbook of Methods in Aquatic Microbial Ecology*. Routledge.

Kim, S., Kang, Y., Kim, H., Yih, W., Coats, D., & Park, M. (2008). Growth and grazing responses of the mixotrophic dinoflagellate Dinophysis acuminata as functions of light intensity and prey concentration. *Aquatic Microbial Ecology*, *51*, 301–310. https://doi.org/10.3354/ame01203

Kishi, M. J., Kashiwai, M., Ware, D. M., Megrey, B. A., Eslinger, D. L., Werner, F. E., Noguchi-Aita, M., Azumaya, T., Fujii, M., Hashimoto, S., Huang, D., Iizumi, H., Ishida, Y., Kang, S., Kantakov, G. A., Kim, H., Komatsu, K., Navrotsky, V. V., Smith, S. L., … Zvalinsky, V. I. (2007). NEMURO—a lower trophic level model for the North Pacific marine ecosystem. *Ecological Modelling*, *202*(1–2), 12–25. https://doi.org/10.1016/j.ecolmodel.2006.08.021

Koch, F., Marcoval, M. A., Panzeca, C., Bruland, K. W., Sañudo-Wilhelmy, S. A., & Gobler, C. J. (2011). The effect of vitamin B $_{12}$ on phytoplankton growth and community structure in the Gulf of Alaska. *Limnology and Oceanography*, *56*(3), 1023–1034. https://doi.org/10.4319/lo.2011.56.3.1023

Leles, S. G., Mitra, A., Flynn, K. J., Stoecker, D. K., Hansen, P. J., Calbet, A., McManus, G. B., Sanders, R. W., Caron, D. A., Not, F., Hallegraeff, G. M., Pitta, P., Raven, J. A., Johnson, M. D., Glibert, P. M., & Våge, S. (2017). Oceanic protists with different forms of acquired phototrophy display contrasting biogeographies and abundance. *Proceedings of the Royal Society B: Biological Sciences*, *284*(1860), 20170664. https://doi.org/10.1098/rspb.2017.0664

Li, A., Stoecker, D. K., & Coats, D. W. (2000). Mixotrophy in gyrodinium galatheanum (dinophyceae): Grazing responses to light intensity and inorganic nutrients. *Journal of Phycology*, *36*(1), 33–45. https://doi.org/10.1046/j.1529-8817.2000.98076.x

Li, Q., Edwards, K. F., Schvarcz, C. R., Selph, K. E., & Steward, G. F. (2020). Plasticity in the grazing ecophysiology of *Florenciella* (Dichtyochophyceae), a mixotrophic nanoflagellate that consumes *Prochlorococcus* and other bacteria. *Limnology and Oceanography*, lno.11585. https://doi.org/10.1002/lno.11585

Lin, S., Litaker, R. W., & Sunda, W. G. (2016). Phosphorus physiological ecology and molecular mechanisms in marine phytoplankton. *Journal of Phycology*, *52*(1), 10–36. https://doi.org/10.1111/jpy.12365

Litzow, M. A., Hunsicker, M. E., Ward, E. J., Anderson, S. C., Gao, J., Zador, S. G., Batten, S., Dressel, S. C., Duffy-Anderson, J., Fergusson, E., Hopcroft, R. R., Laurel, B. J., & O'Malley, R.

(2020). Evaluating ecosystem change as Gulf of Alaska temperature exceeds the limits of preindustrial variability. *Progress in Oceanography*, *186*, 102393. https://doi.org/10.1016/j.pocean.2020.102393

Liu, H., Bidigare, R., Laws, E., Landry, M., & Campbell, L. (1999). Cell cycle and physiological characteristics of Synechococcus (WH7803) in chemostat culture. *Marine Ecology Progress Series*, *189*, 17–25. https://doi.org/10.3354/meps189017

Livanou, E., Barsakis, K., Psarra, S., & Lika, K. (2020). Modelling the nutritional strategies in mixotrophic nanoflagellates. *Ecological Modelling*, *428*, 109053. https://doi.org/10.1016/j.ecolmodel.2020.109053

Livanou, E., Lagaria, A., Santi, I., Mandalakis, M., Pavlidou, A., Lika, K., & Psarra, S. (2019). Pigmented and heterotrophic nanoflagellates: Abundance and grazing on prokaryotic picoplankton in the ultra-oligotrophic Eastern Mediterranean Sea. *Deep Sea Research Part II: Topical Studies in Oceanography*, *164*, 100–111. https://doi.org/10.1016/j.dsr2.2019.04.007

Martin, J. H., & Fitzwater, S. E. (1988). Iron deficiency limits phytoplankton growth in the north-east Pacific subarctic. *Nature*, *331*(6154), 341–343. https://doi.org/10.1038/331341a0

Millette, N. C., Pierson, J. J., Aceves, A., & Stoecker, D. K. (2017). Mixotrophy in *Heterocapsa rotundata*: A mechanism for dominating the winter phytoplankton: Mixotrophy in *Heterocapsa rotundata*. *Limnology and Oceanography*, *62*(2), 836–845. https://doi.org/10.1002/lno.10470

Mitra, A., Flynn, K. J., Tillmann, U., Raven, J. A., Caron, D., Stoecker, D. K., Not, F., Hansen, P. J., Hallegraeff, G., Sanders, R., Wilken, S., McManus, G., Johnson, M., Pitta, P., Våge, S., Berge, T., Calbet, A., Thingstad, F., Jeong, H. J., … Lundgren, V. (2016). Defining Planktonic Protist Functional Groups on Mechanisms for Energy and Nutrient Acquisition: Incorporation of Diverse Mixotrophic Strategies. *Protist*, *167*(2), 106–120. https://doi.org/10.1016/j.protis.2016.01.003

Pinchuk, A. I., Coyle, K. O., & Hopcroft, R. R. (2008). Climate-related variability in abundance and reproduction of euphausiids in the northern Gulf of Alaska in 1998–2003. *Progress in Oceanography*, *77*(2–3), 203–216. https://doi.org/10.1016/j.pocean.2008.03.012

R Core Team (2020). R: A language and environment for statistical computing. R Foundation for Statistical Computing, Vienna, Austria. URL https://www.R-project.org/.

Sanders, R., Berninger, U., Lim, E., Kemp, P., & Caron, D. (2000). Heterotrophic and mixotrophic nanoplankton predation on picoplankton in the Sargasso Sea and on Georges Bank. *Marine Ecology Progress Series*, *192*, 103–118. https://doi.org/10.3354/meps192103

Sato, M., Shiozaki, T., & Hashihama, F. (2017). Distribution of mixotrophic nanoflagellates along the latitudinal transect of the central North Pacific. *Journal of Oceanography*, *73*(2), 159–168. https://doi.org/10.1007/s10872-016-0393-x

Schmidt, K., Birchill, A. J., Atkinson, A., Brewin, R. J. W., Clark, J. R., Hickman, A. E., Johns, D. G., Lohan, M. C., Milne, A., Pardo, S., Polimene, L., Smyth, T. J., Tarran, G. A., Widdicombe,

C. E., Woodward, E. M. S., & Ussher, S. J. (2020). Increasing picocyanobacteria success in shelf waters contributes to long-term food web degradation. *Global Change Biology*, *26*(10), 5574–5587. https://doi.org/10.1111/gcb.15161

Schoener, D. M., & McManus, G. B. (2017). Growth, grazing, and inorganic C and N uptake in a mixotrophic and a heterotrophic ciliate. *Journal of Plankton Research*, *39*(3), 379–391. https://doi.org/10.1093/plankt/fbx014

Smalley, G., Coats, D., & Stoecker, D. (2003). Feeding in the mixotrophic dinoflagellate Ceratium furca is influenced by intracellular nutrient concentrations. *Marine Ecology Progress Series*, *262*, 137–151. https://doi.org/10.3354/meps262137

Stabeno, P. J., Bond, N. A., Hermann, A. J., Kachel, N. B., Mordy, C. W., & Overland, J. E. (2004). Meteorology and oceanography of the Northern Gulf of Alaska. *Continental Shelf Research*, *24*(7–8), 859–897. https://doi.org/10.1016/j.csr.2004.02.007

Stoecker, D. K., Hansen, P. J., Caron, D. A., & Mitra, A. (2017). Mixotrophy in the Marine Plankton. *Annual Review of Marine Science*, *9*(1), 311–335. https://doi.org/10.1146/annurev-marine-010816-060617

Stoecker, D., Li, A., Coats, D., Gustafson, D., & Nannen, M. (1997). Mixotrophy in the dinoflagellate Prorocentrum minimum. *Marine Ecology Progress Series*, *152*, 1–12. https://doi.org/10.3354/meps152001

Stramski, D., Shalapyonok, A., & Reynolds, R. A. (1995). Optical characterization of the oceanic unicellular cyanobacterium *Synechococcus* grown under a day-night cycle in natural irradiance. *Journal of Geophysical Research*, *100*(C7), 13295. https://doi.org/10.1029/95JC00452

Strom, S. L., Fredrickson, K. A., & Bright, K. J. (2016). Spring phytoplankton in the eastern coastal Gulf of Alaska: Photosynthesis and production during high and low bloom years. *Deep Sea Research Part II: Topical Studies in Oceanography*, *132*, 107–121. https://doi.org/10.1016/j.dsr2.2015.05.003

Strom, S. L., Fredrickson, K. A., & Bright, K. J. (2019). Microzooplankton in the coastal Gulf of Alaska: Regional, seasonal and interannual variations. *Deep Sea Research Part II: Topical Studies in Oceanography*, *165*, 192–202. https://doi.org/10.1016/j.dsr2.2018.07.012

Strom, S., Olson, M., Macri, E., & Mord, C. (2006). Cross-shelf gradients in phytoplankton community structure, nutrient utilization, and growth rate in the coastal Gulf of Alaska. *Marine Ecology Progress Series*, *328*, 75–92. https://doi.org/10.3354/meps328075

Tsai, A., Gong, G., Sanders, R., Chen, W., Chao, C., & Chiang, K. (2011). Importance of bacterivory by pigmented and heterotrophic nanoflagellates during the warm season in a subtropical western Pacific coastal ecosystem. *Aquatic Microbial Ecology*, *63*(1), 9–18. https://doi.org/10.3354/ame01470

Unrein, F., Gasol, J. M., Not, F., Forn, I., & Massana, R. (2014). Mixotrophic haptophytes are key bacterial grazers in oligotrophic coastal waters. *The ISME Journal*, *8*(1), 164–176. https://doi.org/10.1038/ismej.2013.132

Unrein, F., Massana, R., Alonso-Sáez, L., & Gasol, J. M. (2007). Significant year-round effect of small mixotrophic flagellates on bacterioplankton in an oligotrophic coastal system. *Limnology and Oceanography*, *52*(1), 456–469. https://doi.org/10.4319/lo.2007.52.1.0456

Verity, P. G., Robertson, C. Y., Tronzo, C. R., Andrews, M. G., Nelson, J. R., & Sieracki, M. E. (1992). Relationships between cell volume and the carbon and nitrogen content of marine photosynthetic nanoplankton. *Limnology and Oceanography*, *37*(7), 1434–1446. https://doi.org/10.4319/lo.1992.37.7.1434

Ward, B. A., & Follows, M. J. (2016). Marine mixotrophy increases trophic transfer efficiency, mean organism size, and vertical carbon flux. *Proceedings of the National Academy of Sciences*, *113*(11), 2958–2963. https://doi.org/10.1073/pnas.1517118113

Wu, J., Aguilar-Islas, A., Rember, R., Weingartner, T., Danielson, S., & Whitledge, T. (2009). Size-fractionated iron distribution on the northern Gulf of Alaska. *Geophysical Research Letters*, *36*(11), L11606. https://doi.org/10.1029/2009GL038304

Supplementary Materials

Supplementary Table 1. Experiment treatments and final values encompassing ambient conditions and any nutrient carryover from prey addition. Light level corresponds to the level of neutral density screening, where the 1.0 level corresponds to no screening (i.e. full proportion of ambient deckboard PAR) and the 0 level corresponds to full coverage with black tape (i.e. 0 proportion of ambient PAR). *Synechococcus* prey concentrations (cells/ml) and nitrate and phosphate concentrations (μM) were calculated by knowing the amount in a spike volume and using that value to calculate the concentration in bottles that received different volumes of the same source culture/nutrient stock.

Station	Exp Type	*Synechococcus* Added	Nitrate Added	Phosphate Added	Light Level	Final *Synechococcus*	Final Nitrate	Final Phosphate	Final PAR Dose
GAK 15	DIN	5.86E+05	4.28	0.33	0.50	6.30E+05	5.25	0.72	4.07
GAK 15	DIN	5.86E+05	2.31	0.17	0.50	6.30E+05	3.27	0.56	4.07
GAK 15	DIN	5.86E+05	1.32	0.08	0.50	6.30E+05	2.28	0.47	4.07
GAK 15	DIN	5.86E+05	0.82	0.04	0.50	6.30E+05	1.79	0.43	4.07
GAK 15	DIN	5.86E+05	0.58	0.02	0.50	6.30E+05	1.54	0.41	4.07
GAK 15	DIN	5.86E+05	0.33	0.00	0.50	6.30E+05	1.29	0.39	4.07
GAK 5	DIN	2.34E+05	6.61	0.28	0.50	4.55E+05	6.93	0.68	4.58
GAK 5	DIN	2.34E+05	3.48	0.14	0.50	4.55E+05	3.80	0.54	4.58
GAK 5	DIN	2.34E+05	1.91	0.06	0.50	4.55E+05	2.23	0.46	4.58
GAK 5	DIN	2.34E+05	1.13	0.03	0.50	4.55E+05	1.45	0.43	4.58
GAK 5	DIN	2.34E+05	0.73	0.01	0.50	4.55E+05	1.05	0.41	4.58
GAK 5	DIN	2.34E+05	0.34	0.00	0.50	4.55E+05	0.66	0.40	4.58
GAK 9	DIN	5.81E+05	7.12	0.43	0.50	1.06E+06	8.55	0.84	4.67
GAK 9	DIN	5.81E+05	3.98	0.22	0.50	1.06E+06	5.42	0.62	4.67
GAK 9	DIN	5.81E+05	2.42	0.11	0.50	1.06E+06	3.85	0.52	4.67
GAK 9	DIN	5.81E+05	1.63	0.06	0.50	1.06E+06	3.06	0.47	4.67
GAK 9	DIN	5.81E+05	1.24	0.03	0.50	1.06E+06	2.67	0.44	4.67
GAK 9	DIN	5.81E+05	0.85	0.01	0.50	1.06E+06	2.28	0.41	4.67
KOD 3	DIN	4.78E+04	6.88	0.46	0.50	7.73E+04	7.36	0.88	1.93
KOD 3	DIN	4.78E+04	3.44	0.23	0.50	7.73E+04	3.92	0.65	1.93
KOD 3	DIN	4.78E+04	1.72	0.11	0.50	7.73E+04	2.20	0.54	1.93
KOD 3	DIN	4.78E+04	0.86	0.06	0.50	7.73E+04	1.34	0.48	1.93
KOD 3	DIN	4.78E+04	0.43	0.03	0.50	7.73E+04	0.91	0.45	1.93
KOD 3	DIN	4.78E+04	0.00	0.00	0.50	7.73E+04	0.48	0.43	1.93
KOD 8	DIN	5.68E+04	7.00	0.35	0.50	2.20E+05	7.45	0.76	6.98
KOD 8	DIN	5.68E+04	3.55	0.17	0.50	2.20E+05	4.01	0.58	6.98

KOD 8	DIN	5.68E+04	1.83	0.09	0.50	2.20E+05	2.28	0.50	6.98
KOD 8	DIN	5.68E+04	0.96	0.04	0.50	2.20E+05	1.42	0.45	6.98
KOD 8	DIN	5.68E+04	0.53	0.02	0.50	2.20E+05	0.99	0.43	6.98
KOD 8	DIN	5.68E+04	0.10	0.00	0.50	2.20E+05	0.56	0.41	6.98
MID 5	DIN	6.43E+05	7.34	0.39	0.50	7.56E+05	7.56	0.64	3.83
MID 5	DIN	6.43E+05	4.67	0.21	0.50	7.56E+05	4.90	0.46	3.83
MID 5	DIN	6.43E+05	3.34	0.12	0.50	7.56E+05	3.56	0.37	3.83
MID 5	DIN	6.43E+05	2.67	0.07	0.50	7.56E+05	2.90	0.33	3.83
MID 5	DIN	6.43E+05	2.34	0.05	0.50	7.56E+05	2.56	0.31	3.83
MID 5	DIN	6.43E+05	2.01	0.03	0.50	7.56E+05	2.23	0.28	3.83
PWS 2	DIN	4.30E+05	7.26	0.49	0.50	4.62E+05	7.33	0.61	5.50
PWS 2	DIN	4.30E+05	3.98	0.25	0.50	4.62E+05	4.05	0.37	5.50
PWS 2	DIN	4.30E+05	2.34	0.13	0.50	4.62E+05	2.41	0.25	5.50
PWS 2	DIN	4.30E+05	1.52	0.07	0.50	4.62E+05	1.59	0.19	5.50
PWS 2	DIN	4.30E+05	1.11	0.04	0.50	4.62E+05	1.19	0.16	5.50
PWS 2	DIN	4.30E+05	0.71	0.01	0.50	4.62E+05	0.78	0.13	5.50
GAK 15	Light	5.86E+05	0.33	0.00	1.00	6.30E+05	1.29	0.38	8.13
GAK 15	Light	5.86E+05	0.33	0.00	0.50	6.30E+05	1.29	0.38	4.07
GAK 15	Light	5.86E+05	0.33	0.00	0.30	6.30E+05	1.29	0.38	2.44
GAK 15	Light	5.86E+05	0.33	0.00	0.10	6.30E+05	1.29	0.38	0.81
GAK 15	Light	5.86E+05	0.33	0.00	0.00	6.30E+05	1.29	0.38	0.00
GAK 5	Light	2.34E+05	0.34	0.00	1.00	4.55E+05	0.66	0.40	9.17
GAK 5	Light	2.34E+05	0.34	0.00	0.50	4.55E+05	0.66	0.40	4.58
GAK 5	Light	2.34E+05	0.34	0.00	0.30	4.55E+05	0.66	0.40	2.75
GAK 5	Light	2.34E+05	0.34	0.00	0.10	4.55E+05	0.66	0.40	0.92
GAK 5	Light	2.34E+05	0.34	0.00	0.00	4.55E+05	0.66	0.40	0.00
GAK 9	Light	5.81E+05	0.85	0.01	1.00	1.06E+06	2.28	0.41	9.35
GAK 9	Light	5.81E+05	0.85	0.01	0.50	1.06E+06	2.28	0.41	4.67
GAK 9	Light	5.81E+05	0.85	0.01	0.30	1.06E+06	2.28	0.41	2.80
GAK 9	Light	5.81E+05	0.85	0.01	0.10	1.06E+06	2.28	0.41	0.93
GAK 9	Light	5.81E+05	0.85	0.01	0.00	1.06E+06	2.28	0.41	0.00
KOD 3	Light	4.78E+04	0.00	0.00	1.00	7.73E+04	0.48	0.43	3.85
KOD 3	Light	4.78E+04	0.00	0.00	0.50	7.73E+04	0.48	0.43	1.93
KOD 3	Light	4.78E+04	0.00	0.00	0.30	7.73E+04	0.48	0.43	1.16
KOD 3	Light	4.78E+04	0.00	0.00	0.10	7.73E+04	0.48	0.43	0.39
KOD 3	Light	4.78E+04	0.00	0.00	0.00	7.73E+04	0.48	0.43	0.00
KOD 8	Light	5.68E+04	0.10	0.00	1.00	2.20E+05	0.56	0.41	13.95
KOD 8	Light	5.68E+04	0.10	0.00	0.50	2.20E+05	0.56	0.41	6.98
KOD 8	Light	5.68E+04	0.10	0.00	0.30	2.20E+05	0.56	0.41	4.19
KOD 8	Light	5.68E+04	0.10	0.00	0.10	2.20E+05	0.56	0.41	1.40

KOD 8	Light	5.68E+04	0.10	0.00	0.00	2.20E+05	0.56	0.41	0.00
MID 5	Light	6.27E+05	2.01	0.03	1.00	7.40E+05	2.23	0.28	7.67
MID 5	Light	6.27E+05	2.01	0.03	0.50	7.40E+05	2.23	0.28	3.83
MID 5	Light	6.27E+05	2.01	0.03	0.30	7.40E+05	2.23	0.28	2.30
MID 5	Light	6.27E+05	2.01	0.03	0.10	7.40E+05	2.23	0.28	0.77
MID 5	Light	6.27E+05	2.01	0.03	0.00	7.40E+05	2.23	0.28	0.00
PWS 2	Light	4.30E+05	0.71	0.01	1.00	4.62E+05	0.78	0.13	11.00
PWS 2	Light	4.30E+05	0.71	0.01	0.50	4.62E+05	0.78	0.13	5.50
PWS 2	Light	4.30E+05	0.71	0.01	0.30	4.62E+05	0.78	0.13	3.30
PWS 2	Light	4.30E+05	0.71	0.01	0.10	4.62E+05	0.78	0.13	1.10
PWS 2	Light	4.30E+05	0.71	0.01	0.00	4.62E+05	0.78	0.13	0.00
GAK 15	Prey	1.17E+06	0.66	0.00	0.50	1.21E+06	1.62	0.39	4.07
GAK 15	Prey	5.86E+05	0.33	0.00	0.50	6.30E+05	1.29	0.39	4.07
GAK 15	Prey	3.53E+05	0.20	0.00	0.50	3.97E+05	1.16	0.39	4.07
GAK 15	Prey	1.20E+05	0.07	0.00	0.50	1.64E+05	1.03	0.39	4.07
GAK 15	Prey	0.00E+00	0.00	0.00	0.50	4.43E+04	0.96	0.39	4.07
GAK 5	Prey	4.74E+05	0.68	0.00	0.50	6.95E+05	1.00	0.40	4.58
GAK 5	Prey	2.34E+05	0.34	0.00	0.50	4.55E+05	0.66	0.40	4.58
GAK 5	Prey	1.42E+05	0.21	0.00	0.50	3.62E+05	0.52	0.40	4.58
GAK 5	Prey	4.91E+04	0.07	0.00	0.50	2.69E+05	0.39	0.40	4.58
GAK 5	Prey	0.00E+00	0.00	0.00	0.50	2.20E+05	0.00	0.40	4.58
GAK 9	Prey	1.16E+06	1.70	0.01	0.50	1.64E+06	3.13	0.42	4.67
GAK 9	Prey	5.81E+05	0.85	0.01	0.50	1.06E+06	2.28	0.41	4.67
GAK 9	Prey	3.47E+05	0.51	0.00	0.50	8.28E+05	1.94	0.41	4.67
GAK 9	Prey	1.14E+05	0.17	0.00	0.50	5.94E+05	1.60	0.41	4.67
GAK 9	Prey	0.00E+00	0.00	0.00	0.50	4.80E+05	0.00	0.00	4.67
KOD 3	Prey	9.56E+04	0.00	0.00	0.50	1.25E+05	0.48	0.43	1.93
KOD 3	Prey	4.78E+04	0.00	0.00	0.50	7.73E+04	0.48	0.43	1.93
KOD 3	Prey	2.84E+04	0.00	0.00	0.50	5.79E+04	0.48	0.43	1.93
KOD 3	Prey	9.56E+03	0.00	0.00	0.50	3.90E+04	0.48	0.43	1.93
KOD 3	Prey	0.00E+00	0.00	0.00	0.50	2.95E+04	0.48	0.43	1.93
KOD 8	Prey	1.14E+05	0.20	0.00	0.50	2.77E+05	0.66	0.41	6.98
KOD 8	Prey	5.68E+04	0.10	0.00	0.50	2.20E+05	0.56	0.41	6.98
KOD 8	Prey	3.43E+04	0.06	0.00	0.50	1.97E+05	0.52	0.41	6.98
KOD 8	Prey	1.14E+04	0.02	0.00	0.50	1.74E+05	0.48	0.41	6.98
KOD 8	Prey	0.00E+00	0.00	0.00	0.50	1.63E+05	0.46	0.41	6.98

Supplementary Table 2. Kendall's tau correlation coefficients for relationships between ambient environmental factors. Fall and summer samples are included. Asterisks indicate significance (alpha = 0.05). Highly correlated values are shown here but were removed from analysis (Nitrate-Nitrite).

	Nitrate	Nitrite	Phosphate	Ammonium	Temperature	Salinity	Par	*Synechococcus*
Nitrate	-	0.924*	0.729*	0.128	-0.498*	0.299	-0.135	-0.012
Nitrite		-	0.740*	0.210	-0.498*	0.259*	-0.126	-0.152
Phosphate			-	0.142	-0.437*	0.585*	0.048	0.065
Ammonium				-	-0.077	0.138	0.286*	0.037
Temperature					-	-0.564*	0.306	-0.101
Salinity						-	0.066	0.257
PAR							-	-0.070
Synechococcus								-

Supplementary Table 3. Kendall's tau correlation coefficients and p-values for correlations between environmental variables ambient fraction feeding by nanoflagellates, dinoflagellates and cryptophytes. Fall and summer data were combined for analysis. The sample size for each group is listed. *: correlation significant at alpha = 0.1; **: correlation significant at alpha=0.05.

	Nanoflagellates (n=33)		Dinoflagellates (n=19)		Cryptophytes (n=9)	
	p-value	tau	p-value	tau	p-value	tau
Salinity	0.218	-0.155	0.830	-0.038	0.600	-0.141
Temperature	0.651	0.057	0.018**	-0.418	0.463	0.197
Nitrate	0.151	0.181	0.857	0.032	0.673	-0.114
Phosphate	0.059*	-0.240	0.774	0.051	0.463	-0.197
Ammonium	0.261	-0.142	0.6408	0.083	0.833	-0.057
Synechococcus	0.055*	0.243	0.173	0.241	0.116	0.423

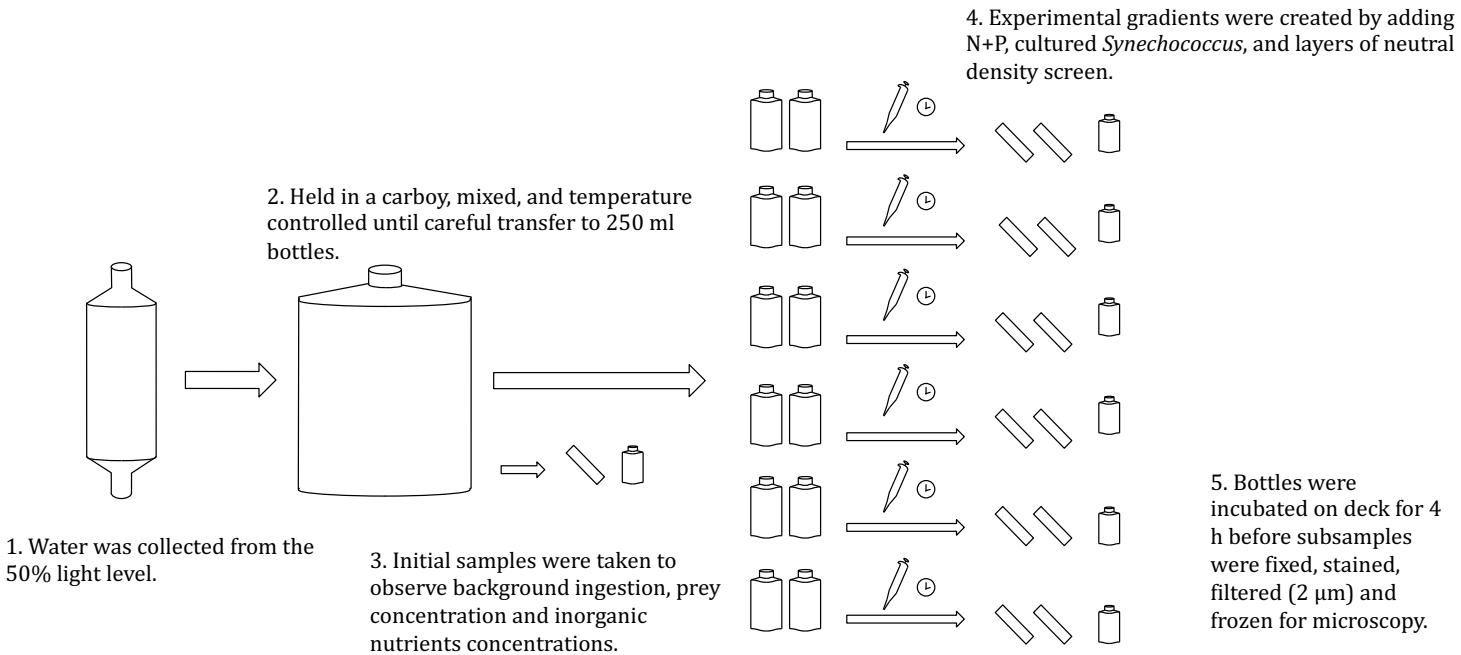

Supplementary Figure 1. Schematic diagram of water collection and experimental design for deckboard incubation experiments.